European Journal of Medicinal Chemistry 143 (2018) 1563–1577

Contents lists available at ScienceDirect

European Journal of Medicinal Chemistry

journal homepage: http://www.elsevier.com/locate/ejmech

Research paper

Design, synthesis and biological evaluation of new β-carboline-bisindole compounds as DNA binding, photocleavage agents and topoisomerase I inhibitors

Jeshma Kovvuri [a, b], Burri Nagaraju [a, b], V. Lakshma Nayak [b], Ravikumar Akunuri [d], M.P. Narasimha Rao [b], Ayyappan Ajitha [c], Narayan Nagesh [c, **], Ahmed Kamal [a, b, d, e, *]

[a] Academy of Scientific and Innovative Research (AcSIR), New Delhi 110025, India
[b] Medicinal Chemistry and Pharmacology Division, CSIR-Indian Institute of Chemical Technology, Hyderabad 500007, India
[c] Centre for Cellular and Molecular Biology, Hyderabad 500007, India
[d] National Institute of Pharmaceutical Education and Research (NIPER), Hyderabad 500 037, India
[e] School of Pharmaceutical Education and Research, Jamia Hamdard University, New Delhi 110062, India

ARTICLE INFO

Article history:
Received 10 September 2017
Received in revised form
16 October 2017
Accepted 17 October 2017
Available online 23 October 2017

Keywords:
β-Carboline
Bis-indole
Topoisomerase I
Antiproliferative activity
DNA-binding affinity
Photocleavage

ABSTRACT

A series of new β-carboline-bisindole compounds were designed, synthesized and evaluated for their antiproliferative activity against human cancer cell lines, such as A549 (lung cancer), DU-145 (prostate cancer), HeLa (cervical cancer) and MCF-7 (breast cancer). All the compounds exhibited considerable antiproliferative activity. Among them, compounds **7g** and **7r** exhibited significant antiproliferative activity against DU-145 cells with IC_{50} values 1.86 and 1.80 μM respectively. Further, these compounds effectively inhibit DNA topoisomerase I activity and can also cleave the pBR322 plasmid upon irradiation with UV light. In addition, Annexin V-FITC assay suggested that these compounds induced apoptosis in DU- 145 cell line (prostate cancer). To know the binding mode of these compounds with DNA, spectroscopic studies were also carried out. These new compounds were showing a unique mode of binding with DNA, both biophysical studies such as UV–Visible, fluorescence, circular dichroism and molecular docking studies revealed that the β-carboline-bisindole compounds exhibit combilexin type of interaction with DNA.

1. Introduction

In the present scenario, cancer has become a global problem with an alarming increase in the number of cancer patients. An estimated 8.2 million deaths are reported in 2012 worldwide, the annual number of new cases due to cancer is projected to rise from 14.1 million in 2012 to 21.6 million by 2030 with an increase in the death rate by 60% [1]. Therefore, enormous efforts are being made to develop affordable and potent cancer chemotherapeutics. Due to the complexity of the disease, success rate of finding a potential candidate is low and multiple biological targets are being pursued to identify a better drug. DNA being the major element involved in cell division and maintenance has been the most important target to develop anticancer drugs [2,3]. The DNA binders are classified into three categories based on their mode of interaction, such as i) intercalators ii) groove binders iii) and combilexins. Combilexin molecules exhibit enhanced DNA interaction with a dual mode of binding compared to single mode [4]. Subsequently, the enzymes associated with the DNA replication and transcription are also important targets for inhibiting the cell proliferation. One such enzyme is a topoisomerase I, which cuts the single strand of DNA double helix and unwinds superhelix of DNA. Studies have revealed that the topoisomerase I is over expressed in tumour cells in comparison to normal cells, due to which this has become an attractive tool for developing anticancer agents [5]. Numerous anticancer drugs containing indolocarbazoles, indenoisoquinolines and camptothecins target topoisomerases [6]. Considering the proximity of this potential target, medicinal chemists have put their efforts to design compounds with combilexin binding for a potential interaction, such as NetAmsa (**I**) that can target DNA as well

* Corresponding author. Medicinal Chemistryand Pharmacology Division, CSIR-Indian Institute of Chemical Technology, Hyderabad 500007, India.
** Corresponding author.
E-mail addresses: nagesh5112@gmail.com (N. Nagesh), ahmedkamal@iict.res.in (A. Kamal).

https://doi.org/10.1016/j.ejmech.2017.10.054
0223-5234/

as topoisomerases to exhibit improved efficacy with greater selectivity [7].

Natural products have played a major role in the quest of developing anticancer drugs [8]. One such class of natural products is β-carboline alkaloids that target tumor cell DNA [9]. These were first isolated from the seeds of *peganum harmala* and exhibit diverse pharmacological properties such as antiplasmodial [10], antimutagenic [11], antiplatelet [12,13] and anticancer [14]. These compounds have been explored extensively due to their multiple physiological effects such as (CDK) [15] cyclin-dependent kinase, (IKK) [16] IkappaB kinase, topoisomerase inhibition [17] and DNA binding ability [18]. Harmine (**II**) is the common representative compound of this family with broad spectrum of cytotoxicity against various cancer cell lines including drug resistant KB sub cells. Due to the planar structure, harmine possesses DNA intercalating ability and inhibits DNA topoisomerase I. The methoxy group present at C-7 position causes neurotoxicity in animals [19] (Fig. 1). Mana-Hox (**III**) is another β-carboline analog that interacts with DNA through intercalation and groove binding, and shows significant cytotoxic activity against various human cancer cell lines including prostate cancer [20]. Considering the importance of β-carbolines, our group has put efforts in designing β-carboline compounds for developing potential DNA binding agents and topoisomerase inhibitors for antiproliferative activity and the studies have shown that the changes in substitutions at C-1 and C-3 positions of β-carboline ring exhibited improved DNA binding ability [21].

On the other hand indoles are the privileged scaffolds with distinct pharmacological properties [22]. Rebeccamycin (**V**), an indolocarbazole, it is an antineoplastic antibiotic. The carbon backbone of rebeccamycin intercalates with DNA and the sugar moiety shows DNA groove binding along with topoisomerase I inhibition [23]. Another bisindole diindoylymethane (DIM) (**IV**), a major component derived from digestion of indole-3-carbinol, has completed the phase II clinical trials for treating patients with stage I and II prostate cancer [24]. DIM bears similar apoptosis inducing property as paclitaxel. In view of β-carboline and indole biological importance a series of β-carboline-bisindole compounds (**7a-z**, **7aa** and **7ab**, Fig. 1) were designed by removing the methoxy group at C-7 and changing various substitutions at C-1 position of β-carboline and introducing substituted bisindoles at the C-3 position for synergistic effect. The synthesized compounds are evaluated for their DNA binding ability and topoisomerase I inhibitory potential.

2. Results and discussion

2.1. Chemistry

The synthetic strategy for the preparation of β-carboline-bisindole compounds (**7a-z, 7aa** and **7ab**) is outlined in the Scheme 1. The L-tryptophan methyl ester **(2)** was prepared by esterification of L-tryptophan **(1)** using $SOCl_2$ and methanol, which was subjected to the Pictet-Spengler condensation with different aldehydes in the presence of catalytic amount of *p*-TSA to get the respective methyltetrahydro-β-carboline-3-carboxylates **(3a-d)**. Compounds **3a-d** were aromatized using trichloroisocyanuric acid to yield methyl-β-carboline-3-carboxylates **(4a-d)**, followed by reduction of **4a-d** with $LiAlH_4$ to obtain the respective carbinols **(5a-d).** Carbinols **5a-d** were oxidized with DMP to furnish the desired methyl-β-carboline-3-carboxaldehyde **(6a-d)**. Here the final reaction of various substituted indoles with the synthesized β-carboline aldehydes (**6a-d**) in the presence water-ethanol solvent mixture, using Amberlite IR-120H as a recyclable heterogeneous catalyst under the reflux conditions offered the desired compounds **7a-z, 7aa** and **7ab** in good to excellent yields. All the compounds were confirmed by ^{1}H, ^{13}C, ESI-MS and HRMS, the purity of the active compounds were demonstrated by HPLC.

2.2. Biological activity

2.2.1. Antiproliferative activity

All the newly synthesized β-carboline-bisindole compounds were evaluated for their antiproliferative activity against human cancer cell lines, such as A549 (lung cancer), DU-145 (prostate cancer), HeLa (cervical cancer) and MCF-7 (breast cancer) using MTT assay. Gratifyingly, the series of compounds (**7a-z, 7aa & 7ab**) exhibited good to moderate cytotoxic activity ranging from 1.80 to 44.20 μM. The cytotoxicity results were expressed as IC_{50} values and the results were summarized in Table 1 compared to positive controls harmine and doxorubicin. Among the synthesized 28 compounds, 11 of the compounds (**7g**, **7i**, **7j, 7m, 7n, 7p**, **7r**, **7t-v**, and **7aa**) exhibited pronounced cytotoxicity against DU-145 cell line. The most active compounds of the series were **7g**, **7r** and **7t** with IC_{50} values of 1.86, 1.80–1.92 μM respectively. The cytotoxicity of the β-carboline-bisindole compounds depend on the nature of substituents on the phenyl ring at C-1 position (R^1, R^2 and R^3, Fig. 2) and on indole moiety at C-3 position (R^4 and R^5).

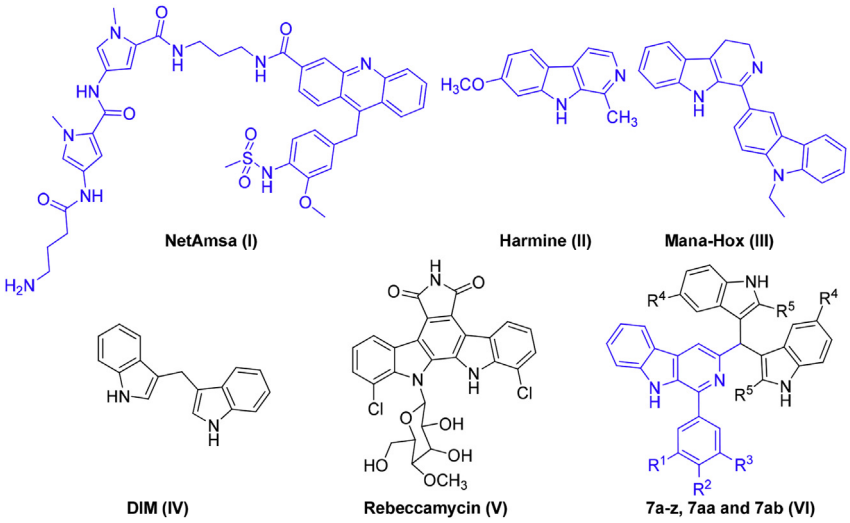

Fig. 1. Chemical structures of a representative example of combilexin (**I**), β-Carboline and bisindole containing bioactive compounds (**II-V**) and designed prototype (**VI**).

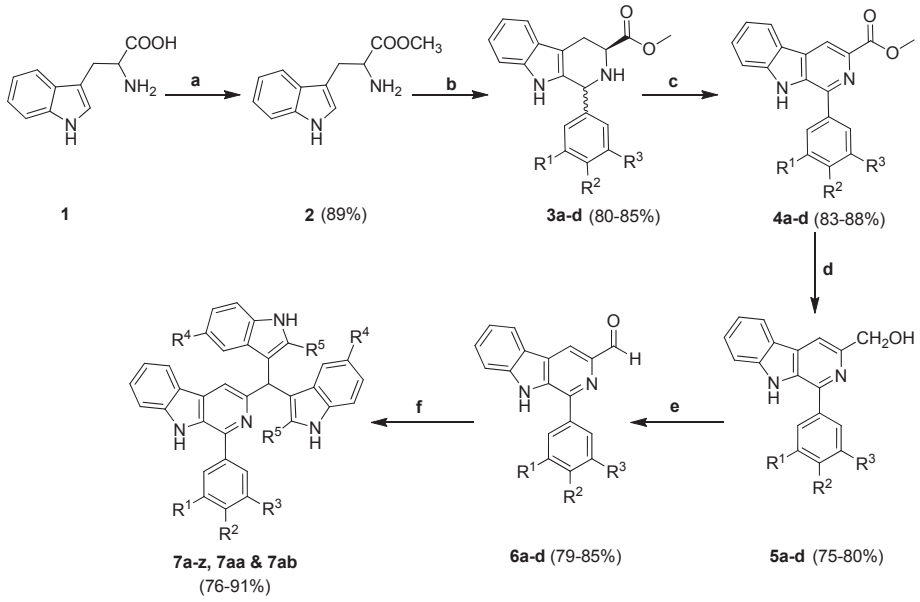

Scheme 1. Synthesis of β-carboline-bisindole derivatives: (a) $SOCl_2$, methanol, 27 °C, 8 h; (B) corresponding aldehyde, cat. *p*-TSA, toluene, 110 °C, 12 h; (c) TCC, DMF, triethylamine, −20 °C; 0–27 °C, 2 h; (d) $LiAlH_4$, dry THF, 0–27 °C, 4 h; (e) DMP, CH_2Cl_2, 27 °C, 2 h; (f) respective indole, water-ethanol, cat. Amberlite IR- 120, 80 °C, 6 h.

Table 1
In vitro antiproliferative activity ([a]IC_{50} in μM) of β-carboline-bisindole compounds in human cancer cell lines.

Entry	R^1	R^2	R^3	R^4	R^5	A549[b]	DU-145[c]	Hela[d]	MCF-7[e]	NIH3T3[f]
7a	OMe	OMe	OMe	Br	H	21.83 ± 1.07	14.67 ± 3.02	15.77 ± 1.17	33.42 ± 3.16	64.34 ± 0.83
7b	OMe	OMe	OMe	H	H	22.65 ± 1.98	12.82 ± 0.72	21.37 ± 0.25	34.92 ± 1.56	92.86 ± 1.81
7c	OMe	OMe	OMe	NO_2	CH_3	31.69 ± 0.81	20.67 ± 1.97	22.63 ± 2.04	33.14 ± 0.73	105.11 ± 2.70
7d	OMe	OMe	OMe	NO_2	H	17.07 ± 1.42	11.86 ± 1.54	14.21 ± 2.70	16.30 ± 1.02	127.75 ± 0.35
7e	OMe	OMe	OMe	CN	H	19.28 ± 1.88	19.00 ± 4.02	9.86 ± 1.08	11.75 ± 1.73	57.25 ± 1.06
7f	H	Me	H	H	H	10.00 ± 0.40	13.66 ± 1.89	14.26 ± 0.57	18.11 ± 2.06	100.80 ± 2.26
7g	H	Me	H	Br	H	2.51 ± 0.31	1.86 ± 0.26	2.54 ± 0.91	5.85 ± 0.66	124.67 ± 0.39
7h	H	Me	H	NO_2	CH_3	21.12 ± 2.95	15.00 ± 0.32	28.07 ± 0.04	22.78 ± 2.71	52.12 ± 3.29
7i	H	Me	H	NO_2	H	6.92 ± 0.13	6.00 ± 1.05	10.88 ± 1.66	16.95 ± 1.42	145.29 ± 1.66
7j	H	Me	H	CN	H	11.04 ± 1.84	7.32 ± 1.02	15.96 ± 1.52	17.42 ± 0.93	60.63 ± 3.04
7k	H	OMe	H	H	H	13.48 ± 1.04	12.81 ± 2.11	26.19 ± 3.79	38.13 ± 1.11	83.18 ± 0.19
7l	H	OMe	H	NO_2	Me	11.66 ± 1.17	16.63 ± 1.04	21.52 ± 2.11	25.27 ± 1.09	125.75 ± 0.70
7m	H	OMe	H	Br	H	9.24 ± 2.83	2.63 ± 0.60	15.00 ± 0.72	18.63 ± 2.70	86.29 ± 1.83
7n	H	OMe	H	NO_2	H	10.44 ± 1.05	9.31 ± 0.99	18.01 ± 1.68	50.11 ± 2.88	118.10 ± 2.58
7o	H	OMe	H	CN	H	13.70 ± 0.21	14.85 ± 2.81	30.93 ± 2.10	28.94 ± 2.86	119.28 ± 0.30
7p	H	OMe	H	F	H	27.55 ± 1.03	8.33 ± 0.83	35.54 ± 0.91	30.57 ± 3.07	94.39 ± 4.72
7q	H	OMe	H	OMe	H	18.05 ± 2.86	16.26 ± 2.71	32.47 ± 1.82	29.93 ± 0.81	101.65 ± 1.20
7r	H	F	H	H	H	2.04 ± 0.71	1.80 ± 0.33	3.25 ± 1.77	8.50 ± 1.04	140.14 ± 3.98
7s	H	F	H	NO_2	Me	18.60 ± 2.17	16.89 ± 1.72	31.50 ± 0.74	27.69 ± 2.01	101.80 ± 1.56
7t	H	F	H	NO_2	H	6.32 ± 0.11	1.92 ± 1.03	12.81 ± 1.11	14.36 ± 2.06	64.18 ± 0.44
7u	H	F	H	CN	H	15.67 ± 2.07	2.34 ± 0.79	17.11 ± 2.76	26.31 ± 2.98	58.05 ± 0.50
7v	H	F	H	Br	H	8.30 ± 1.74	7.74 ± 0.95	9.50 ± 2.03	18.30 ± 2.33	90.08 ± 2.06
7w	H	F	H	F	H	18.50 ± 1.90	15.79 ± 1.65	18.09 ± 2.76	19.81 ± 1.79	113.63 ± 4.30
7x	H	F	H	OMe	H	14.55 ± 0.95	10.56 ± 1.05	23.74 ± 1.11	34.62 ± 1.18	110.26 ± 1.72
7y	OMe	OMe	OMe	F	H	16.91 ± 1.88	10.11 ± 1.10	12.15 ± 1.09	13.60 ± 1.24	118.33 ± 1.82
7z	OMe	OMe	OMe	OMe	H	20.42 ± 2.77	19.46 ± 0.74	39.81 ± 2.61	44.20 ± 1.29	100.20 ± 1.40
7aa	H	Me	H	F	H	14.19 ± 2.02	5.81 ± 1.01	12.38 ± 0.18	14.23 ± 0.02	66.22 ± 0.27
7ab	H	Me	H	OMe	H	30.14 ± 1.79	23.06 ± 1.71	33.75 ± 2.05	27.39 ± 2.00	59.26 ± 2.89
Har[h]						7.76 ± 1.66	12.02 ± 1.92	16.21 ± 1.05	10.78 ± 1.53	ND[g]
Doxo[h]						1.86 ± 0.59	2.13 ± 0.47	1.73 ± 0.70	2.18 ± 0.11	ND[g]

[a] 50% Inhibitory concentration after 48 h of drug treatment and the values are average of three individual experiments.
[b] Lung cancer.
[c] Prostate cancer.
[d] Cervical cancer.
[e] Breast cancer.
[f] Normal cells.
[g] ND: Not determined.
[h] Har = Harmine, Doxo = Doxorubicin.

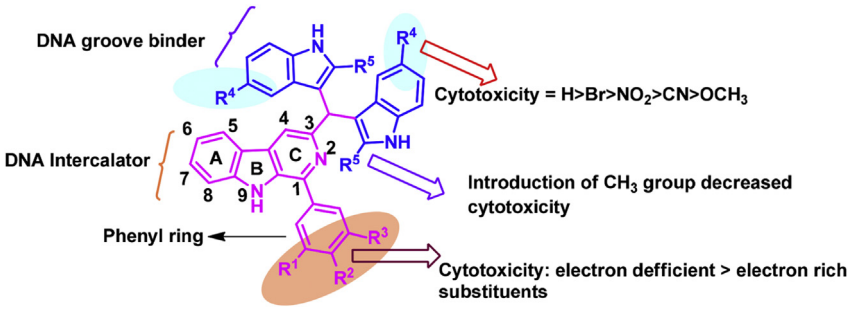

Fig. 2. Structure activity relationship of β-carboline-bisindole compounds.

In order to know SAR of the compounds, different substituents on the phenyl and indole rings were varied. Among all the synthesized compounds 4-Fluoro (**7r** and **7t-7v**) substituent on the phenyl ring at C-1 position displayed potent antiproliferative activity and then followed by 4-methyl (**7g, 7i and 7j**) substituent against DU-145 cells. The number of methoxy substituents on the phenyl ring had a major influence on antitumor activity. Replacement of 4-methyl group (**7g, 7i and 7aa**) on the phenyl ring with more electron rich methoxy group (**7m, 7n** and **7p**) decreased antiproliferative activity by 1.4 folds in the DU-145 cells and three methoxy substituents (**7a**) on the phenyl ring caused a substantial decrease in the antiproliferative activity by 5.6 folds with respective to **7m** compound in the DU-145 cells. We speculate that the electron deficient substituents enhanced cytotoxic activity in comparable to the electron rich substituents. In addition, the influence of C-3 substituents on activity was also examined. 5-unsubstituted indole, electron deficient substituents such as Br, F, CN and NO_2 at C-5 position on indole ring linked to C-3 position of β-carboline enhanced antiproliferative activity, while electron rich OCH_3 group decreased the activity and replacing the hydrogen of indole C-2 position (**7d, 7i, 7n** and **7t**) with the bulky methyl group (**7c, 7h, 7l** and **7s**) leads to decrease in potency by 1.7–8.8 folds in the DU-145 cells, Further, to understand the mode of action, some detailed biological studies were carried out by taking most active compounds based on MTT assay.

2.2.2. DNA topoisomerase I inhibition study

DNA topoisomerase I (topo I) has been identified as the potential target of several anticancer drugs used clinically today. Since topo I is involved in replication and proliferation process, over production of topo I was noticed in cancer cells compared to normal cells. In general, topo I control the changes in the DNA structure by cutting a single stranded DNA and re-joining the phosphate backbone during the normal cell cycle. Mechanism of topo I inhibition is known to occur in two ways, these inhibitors may bind topoisomerase directly or they may bind to DNA and alter its structure, so that it cannot be recognized by topoisomerases. In the present study, the potential of the **7g, 7r** and **7t** compounds towards inhibition of topo I was studied. A well known quinoline alkaloid known for topo I inhibition namely, camptothecin was used as a positive control (shown in lane 6 in Fig. 3). Interestingly, **7g, 7r** and **7t** compounds along with camptothecin have shown significant topo I inhibition at 20 μM concentration (lane 3–5, Fig. 3). All the compounds (**7g**, **7r** and **7t**) were found to inhibit topo I activity.

2.2.3. DNA photocleavage

The DNA photocleavage reaction was carried out in the presence of **7g, 7r** and **7t** compounds to find their efficiency in cleaving pBR322 supercoiled DNA by generating free radicals in the system. In general, the photocleavage reactions proceed via the generation

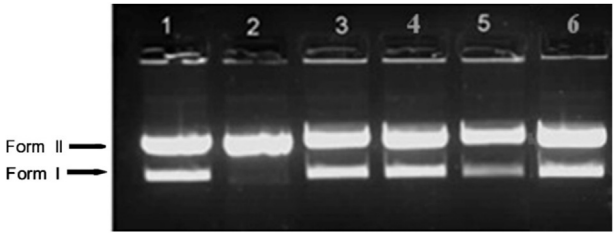

Fig. 3. Agarose gel picture of showing Topoisomerase I inhibition: lane 1: pBR322 DNA alone; lane 2: pBR322 DNA (0.5 μg) with topoisomerase I (1 unit); lane 3: pBR322 DNA with topo I and **7g** (20 μM); lane 4: pBR322 DNA with topo I and **7r** (20 μM); lane 5: pBR322 DNA with topo I and **7t** (20 μM), lane 6: pBR322 DNA with topo I and camptothecin.

of molecular oxygen or hydroxyl radical species. These reactions involve triplet oxygen state ($^3O_2$) that could proceed by two major mechanistic pathways. In the first one, the singlet excited electronic state of the compound through inter system crossing, generate an excited triplet state of the compound which in turn activate the molecular oxygen in its stable triplet oxygen state ($^3O_2$) to a more reactive singlet oxygen state ($^1O_2$) [25]. In an alternate pathway, the excited state molecule could reduce molecular oxygen to generate highly reactive hydroxyl radical. The ability of these compounds (**7g, 7r** and **7t)** to cleave DNA upon irradiation with UV light of 365 nm wavelength followed by agarose gel electrophoresis depicts that they generate free radicals to function as potent photocleavage agents and appear to be suitable for photodynamic therapy (PDT). In the absence of **7g, 7r** and **7t**, when the pBR322 plasmid DNA is subjected to electrophoresis, a dense and relatively fast migration band was noticed in the supercoiled form (Form I). Upon cleaving one strand of supercoiled DNA, it will relax to generate a relaxed circular form (Form II). The gel electrophoresis separation of pBR322 DNA after the addition of **7g, 7r** and **7t** ligands (20 μM) and upon UV-light irradiation for 1 h was shown in Fig. 4. The experimental results indicate that, control (DNA solution alone irradiated) as well as DNA + compounds (20 μM) incubated in the dark did not show cleavage. However, the DNA samples irradiated along with **7g** and **7r** exhibited photocleavage as evidenced by the decrease in the intensity of Form I. Further, **7g** and **7r** are considerably active to generate more free radicals that will effectively cleave the supercoiled DNA. Among **7g** and **7r,** effect of UV-light irradiation on supercoiled DNA cleavage was more in case of **7g** followed by **7r.** Topo I inhibition and UV cleavage experiments indicate that among **7g, 7r** and **7t** compounds, **7g** and **7r** demonstrated maximum potential. **7t** has minimum effect on DNA cleavage in the presence of UV light. Even cytotoxicity data also indicate that **7g** and **7r** are more efficient, so we further carried out experiments only with **7g** and **7r**.

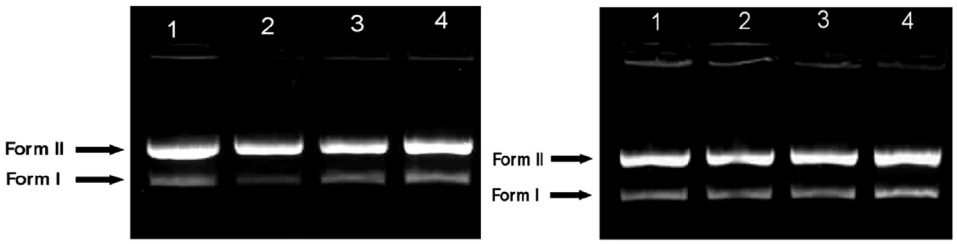

Fig. 4. Gel electrophoresis depicting photocleavage of pBR322 DNA: A) with UV-light irradiation, B) DNA cleavage in absence of UV-light irradiation; lane 1: pBR322 DNA alone (0.45 μg); lane 2: pBR322 DNA with **7g** (20 μM); lane 3: pBR322 DNA with **7r** (20 μM); lane 4: pBR322 DNA with **7t** (20 μM).

2.2.4. Cell cycle analysis

Many anticancer compounds exert their growth inhibitory effect either by arresting the cell cycle at a particular checkpoint of cell cycle or by induction of apoptosis or a combination of both [26,27]. The screening results revealed that compounds **7g** and **7r** showed significant cytotoxic activity against human prostate cancer cell line (DU-145). A cell cycle analysis study was performed, wherein DU-145 cells were treated with these compounds (**7g** and **7r**) for 48 h at 1 μM and 2 μM concentrations respectively. The data obtained clearly indicated that these compounds show cell cycle arrest at G2/M phase in comparison with the untreated control cells. G2/M phase cell cycle arrest is a common cellular response to a variety of DNA-damaging agents [28]. These compounds (**7g** and **7r**) showed 22.04% and 57.46% of cell accumulation in G2/M phase at 1 μM concentration, whereas they exhibited 57.12% and 62.86% of cell accumulation at 2 μM concentration, respectively (Fig. 5 and Table 2).

2.2.5. Apoptosis assay

Induction of apoptosis among DU-145 cell by **7g** and **7r** compounds were evaluated by Annexin V FITC/PI (AV/PI) dual staining assay [29] to examine the occurrence of phosphatidylserine externalization and also to understand whether it is due to physiological apoptosis or nonspecific necrosis. In this study, DU-145 cells were treated with these compounds for 48 h at 1 and 2 μM concentrations to examine the apoptotic effect. It was observed that these compounds showed significant apoptosis against DU-145 cells as shown in Fig. 6. Results indicated that compounds **7g** and **7r** showed 12.86% and 15.04% at 1 μM concentration, whereas they exhibited 35.88% and 43.34% apoptosis at 2 μM concentrations respectively for 48 h (Table 3).

2.2.6. Circular dichroism studies

In order to understand the effect of β-carboline-bisindole compounds on DNA conformation, circular dichroism studies were performed. The CT-DNA shows positive and negative CD bands at 275 nm and 245 nm respectively. At an average all the β-carboline-bisindole compounds demonstrated around 10–12% of positive CD band hypochromicity on interaction with CT DNA. On addition of 10 μM **7g** and **7r** compounds to CT-DNA (at 1:1 ratio), the positive CD band showed hypochromicity, indicating unwinding of CT-DNA on interaction with β-carboline-bisindole compounds. Further, on doubling the concentration of β-carboline-bisindole compounds (at 1:2 ratio), the positive band intensity reduced further and exhibited slight red shift. Red shift of the positive CD band is an indication of good interaction between the bound β-carboline-bisindole compounds and CT-DNA. CD studies indicate that β-carboline-bisindole compounds interact with DNA and they can bring change in DNA conformation. The extent of positive CD band hypochromicity is more with **7r** compared to **7g**. From the CD data it is evident that β-carboline-bisindole compounds alter DNA helix on its interaction with CT-DNA, which is clear from the changed negative CD band intensities. The representative CD spectra obtained with **7g** and **7r** compounds and CT-DNA was shown in Fig. 7.

2.2.7. UV–visible studies

UV–visible studies are useful in understanding the mode of binding of these compounds with DNA. All the complexes has absorption peak at around 370 nm. On addition of equal concentration of CT DNA, the absorption band at 370 nm exhibited hypochromicity without exhibiting any shift. It is known that hypochromicity along with the larger bathochromic shift (red shift) is an evidence of intercalative mode of binding [30]. The extent of hypochromicity of the absorption band can be taken as a measure of intercalative binding strength [31]. The absorption band hypochromicity is usually attributed to the interaction between the electronic states of the complex and the DNA bases [32]. From the results it is evident that the hypochromicity of UV–visible band at 370 nm is comparatively more with **7g** compared to **7r**. This shows that the β-carboline-bisindole compounds show very good interaction with double stranded DNA, may be by intercalative mode. The representative UV–visible spectra obtained on interaction of compounds with CT-DNA are shown in Fig. 8.

2.2.8. Fluorescence titrations

Fluorescence titration is yet another valuable technique for understanding the binding mode of small molecules with DNA and to study the electronic environment around the DNA-complex formed with molecules at comparatively lower concentrations [33]. Since the β-carboline-bisindole compounds are fluorescent, their interaction with DNA can be monitored at low concentration. The emission spectra of these compounds show prominent peaks in the region between 395 nm and 470 nm. On addition of equal increments of DNA to the all the compound solutions, the emission peak intensities decrease gradually. The extent of fluorescence hypochromicity both at 395 nm and 470 nm is slightly higher in case of **7r** compared to **7g**. However, higher fluorescence quenching in case of **7g** and **7r** is probably due to the stacking of the compounds to the surface of DNA [34]. Indeed, simple β-carboline alkaloids such as harmine and harmane are well known DNA intercalators having fully planar nature, whereas the mode of binding of these β-carboline compounds is slightly different that could be due to their structure and planarity. The fluorescence spectra were shown in Fig. 9.

2.2.9. Viscosity studies

In order to clearly understand the nature of interaction of these molecules with CT DNA, viscosity studies were carried out. Spectroscopic studies indicate that they interact well with CT DNA, as the relative viscosity of DNA increases when a molecule intercalate with DNA. The enhancement of viscosity is due to increase in the axial length of DNA helix on molecules intercalation [35]. Whereas, reduction in the relative viscosity is typically observed due to covalent DNA binding [36] and on the other hand the viscosity does

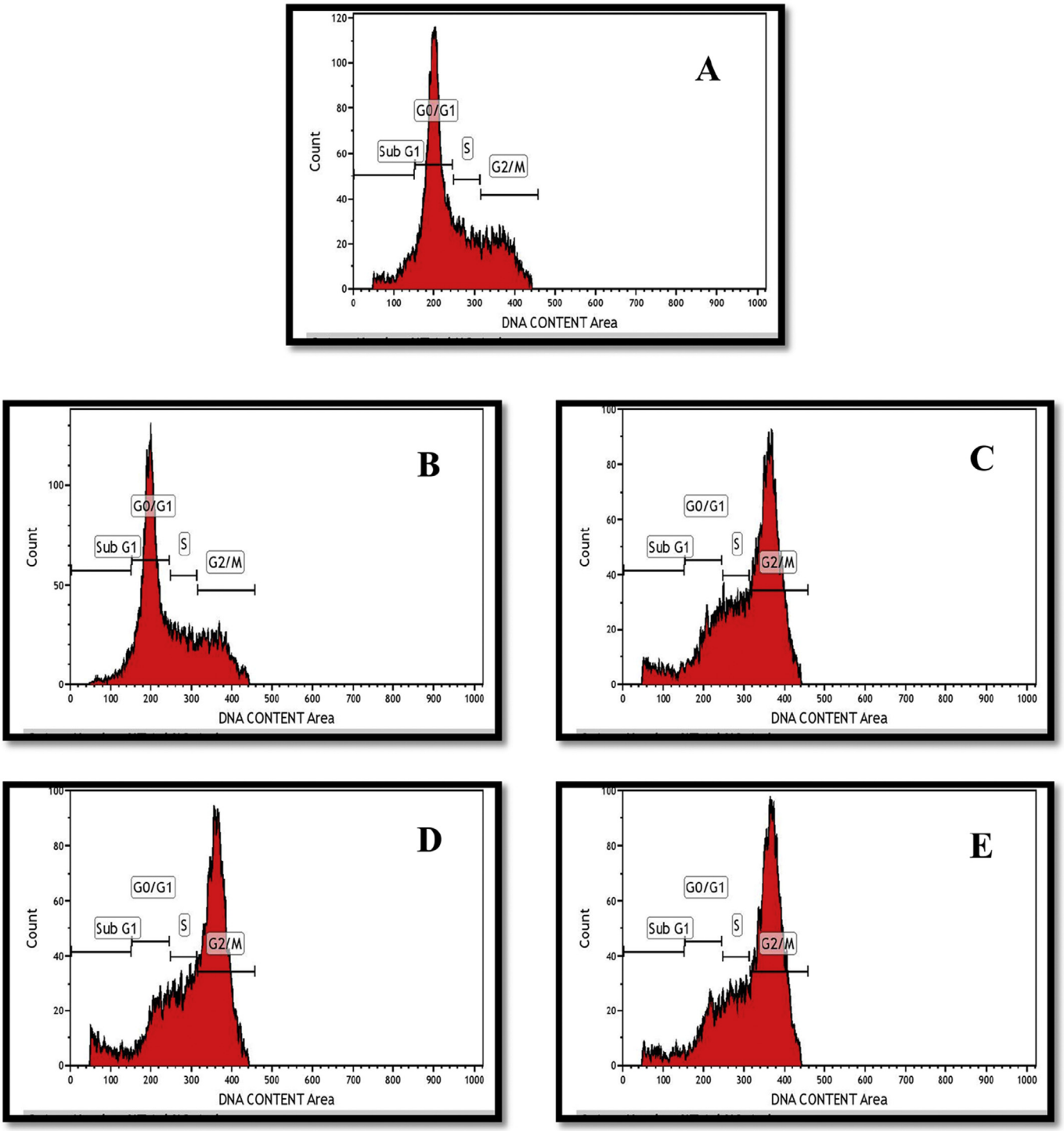

Fig. 5. Flow cytometric analysis in DU-145 cells after treatment with compounds **7g** and **7r** at 1 and 2 μM concentrations for 48 h. A: Control cells, B: **7g** (1 μM), C: **7g** (2 μM), D: **7r** (1 μM) and E: **7r** (2 μM).

Table 2
Effect of compounds**7g** and**7r** on cell cycle phase distribution in DU-145 cells.

Sample	Sub G1%	G0/G1%	S %	G2/M %
A: Control	7.71	53.60	16.22	21.07
B: **7g** (1 μM)	5.57	54.58	16.37	22.04
C: **7g** (2 μM)	6.05	15.92	19.52	57.12
D: **7r** (1 μM)	6.91	15.15	19.16	57.46
E: **7r** (2 μM)	4.93	13.58	17.41	62.86

not change or show very less change when molecules bind to the surface of the DNA. With the addition of **7g** and **7r**, there was a slight enhancement of viscosity in the DNA solution was noticed. Minor positive or negative changes in DNA solution viscosity were observed when binding occurs in the DNA grooves. As shown in Fig. 10, on addition of **7g** and **7r** complexes to CT DNA there is a slight increase in the viscosity, which is in between the classical intercalators like EtBr [37] and the groove-binder like Hoechst

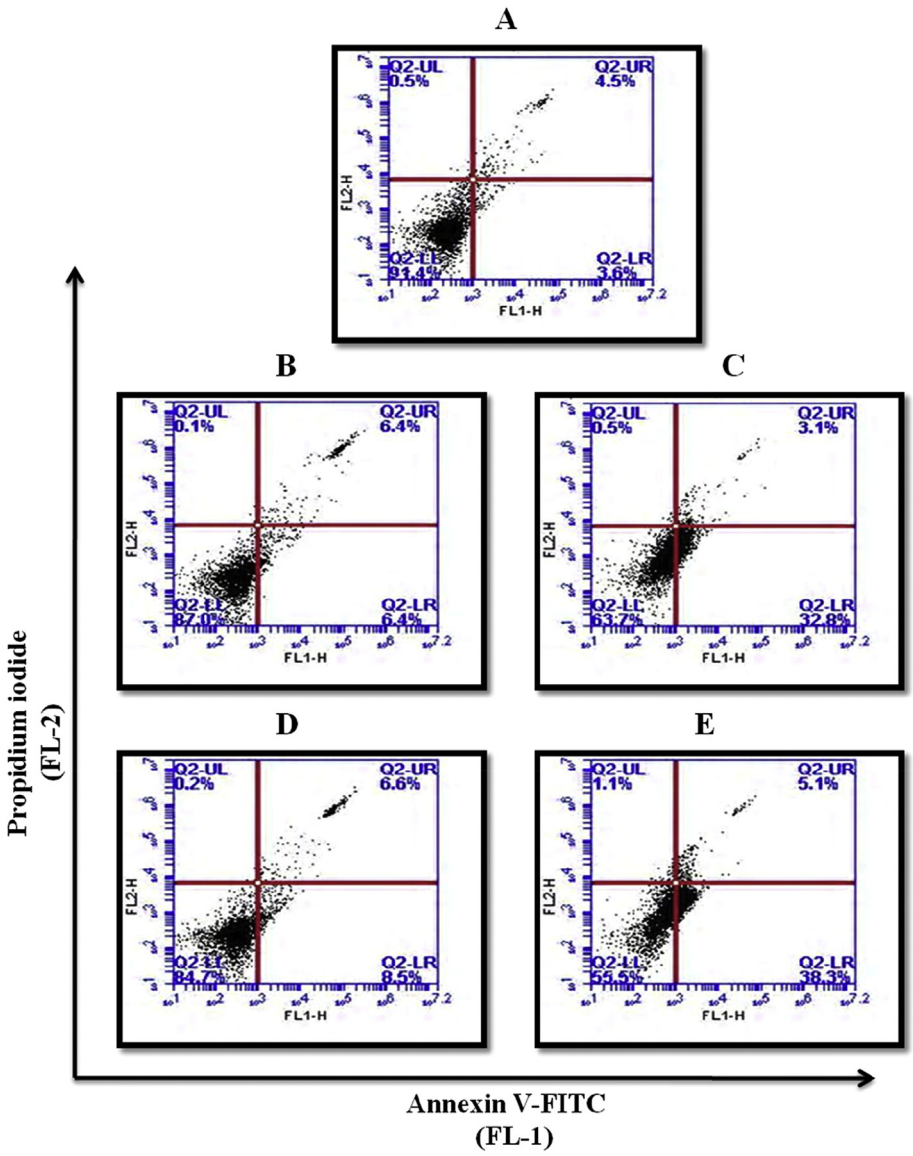

Fig. 6. Annexin V-FITC/PI (AV/PI) dual staining assay: Quadrants; Upper left (necrotic cells), Lower left (live cells), Lower right (early apoptotic cells) and Upper right (late apoptotic cells). A: control cells (DU-145), B: **7g** (1 μM), C: **7g** (2 μM), D: **7r** (1 μM) and E: **7r** (2 μM).

Table 3
Distribution of apoptotic cells in Annexin-V FITC experiment.

Sample	Upper left %	Upper right %	Lower left %	Lower right %
A: Control (DU-145)	0.49	4.46	91.44	3.61
B: **7g** (1 μM)	0.12	6.43	87.01	6.43
C: **7g** (2 μM)	0.47	3.12	63.65	32.76
D: **7r** (1 μM)	0.23	6.55	84.73	8.49
E: **7r** (2 μM)	1.14	5.06	55.52	38.28

33342 [38].

As a control, 5 μM of ethidium bromide (EtBr) and Hoechst 33342 was added to CT-DNA. The viscosity of DNA on addition of EtBr has increased continuously, on the other hand, no change was noticed when Hoechst 33342 was added to CT-DNA. Upon plotting the values, the viscosity graphs with **7g** and **7r** were seen in between ethedium bromide (a strong intercalator) and Hoechst (a known groove binder). From these results it is speculated that they may be exhibited combilexin type of interaction between CT-DNA and **7g/7r** molecules. The graph plotted between $(\eta/\eta_o)^{1/3}$ and complex/CT-DNA was shown in Fig. 10.

2.3. Molecular docking

The β-carboline derivatives of C-1 and C-3 substitutions are exhibiting efficient DNA binding abilities and topoisomerase I inhibition. Biophysical studies speculated that the synthesized β-carboline-bisindole compounds could behave like combilexin-type

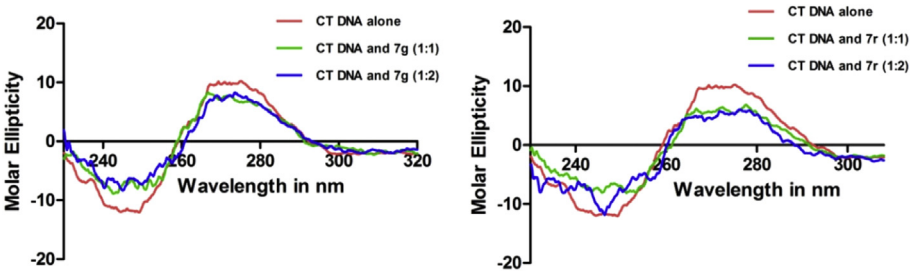

Fig. 7. Circular dichroism spectra represents the CT-DNA (10 μM) at 10.0 μM and 20 μM of compounds **7g** and **7r**.

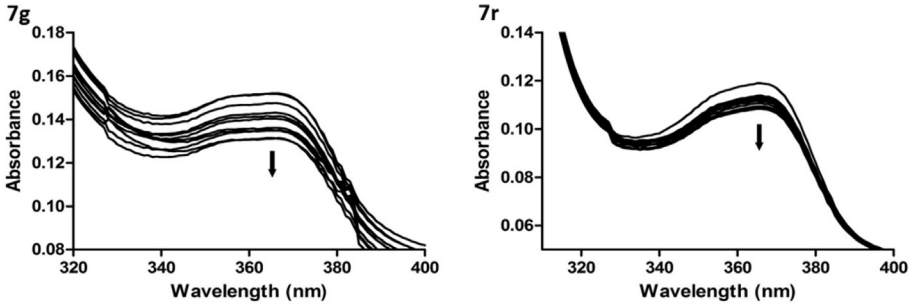

Fig. 8. UV–Visible spectra indicates the interaction of compounds **7g** (1 ml of 25.0 μM) and **7r** (1 ml of 25.0 μM) with the addition of 5 μl of DNA (25.0 μM) each time at 25 °C.

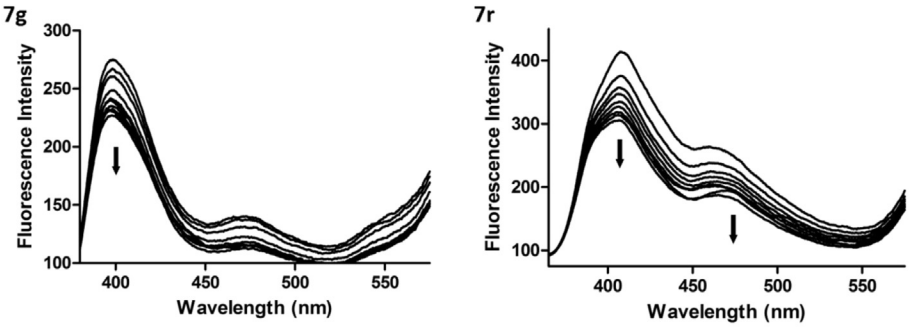

Fig. 9. Fluorescence spectra depicts the interaction of compounds **7g** (10 μM) and **7r** (10 μM) with increasing concentrations of CT-DNA (multiples of 0.5 μM) at 25 °C.

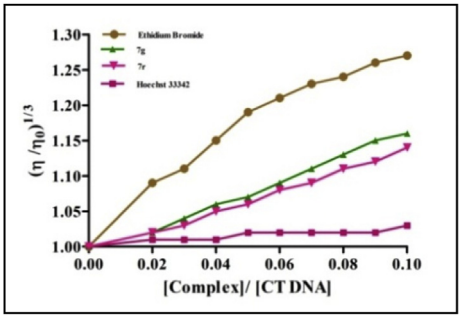

Fig. 10. Viscocity studies graphical representation of **7g** (15 μM) and **7r** (15 μM) compounds with CT-DNA solution (150 μM) at 25 °C, EtBr-CT-DNA and Hoechst 33342-CT-DNA complexes are controls.

of molecules. Hence we chose a pair of crystal structures (PDB IDs: 1SC7 and 1NAB for DNA-Topo-1 inhibition and combilexin-type of binding to DNA respectively) to know the structural details of protein-small molecule complex on interaction with active compounds **7g** and **7r** within the constraints of target protein binding site by molecular docking studies.

These compounds fit well into M38 binding pocket present in DNA-Topo 1 complex (PDB ID: 1SC7), β-carboline ring intercalated with DNA (Fig. 11A) and the C-1 substituents exhibited π-stacking interactions with dT10, TGP11, dC112, dA113 nitrogen bases and hydrophobic interactions with side chains of Arg364, Thr718 and Asn722 amino acid residues (Fig. 11B and C). Whereas the C-3 substituents extended out of the groove and showing hydrophobic interactions with dT10, Ala351, Asn352, Tyr426, Met428 and Lys436. In addition, the same C-3 substituent present in the compounds **7g** and **7r** also interact with Ile427 and dT9 respectively.

Biophysical studies and our previous reports also proved that the C-1 and C-3 substituted β-carboline compounds could behave like combilexin type of molecules [39]. The combilexin type of interaction of **7g** and **7r** compounds with DNA is evaluated using the DNA crystal structure with PDB ID: 1NAB. In this regard, molecular docking of compounds **7g** and **7r** at the 44D binding pocket of DNA (PDB ID: 1NAB) indicates combilexin type of binding (Fig. 12A and B). In which β-carboline ring stacked in between the consecutive DNA base pairs dG12-dC1 and dC11-dG2, C-1 substituents show good interaction with the DNA helices and interacts well with dG-2, dA-3. On the other hand, C-3 substituents showing

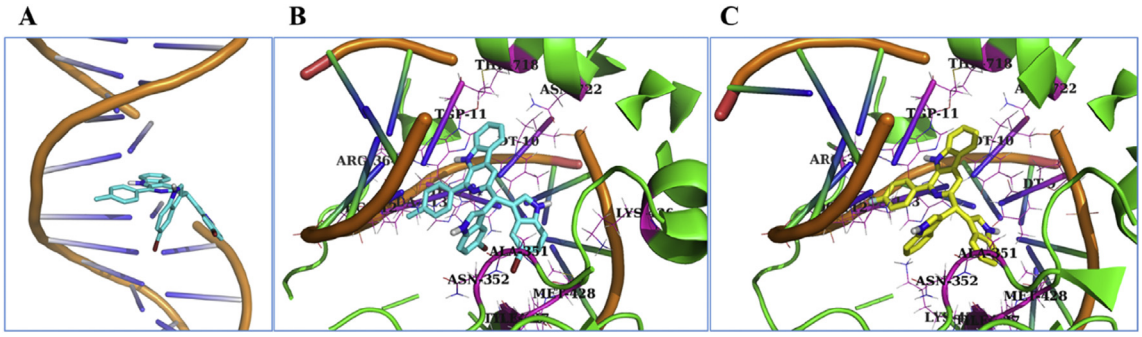

Fig. 11. A) DNA intercalation of compound **7g,** B) and C) Binding pose and hydrophobic interactions of compound **7g** and **7r** respectively in M38 binding pocket of DNA- Topo-1 (PDB ID: 1SC7), where protein is shown as a cartoon representation, compound **7g** and **7r** were shown in stick and coloured by the atom type. Carbon: Cyan (**7g**), yellow (**7r**); Bromine: red; hydrogen: white; nitrogen: blue; fluorine: ice blue). (For interpretation of the references to colour in this figure legend, the reader is referred to the web version of this article.)

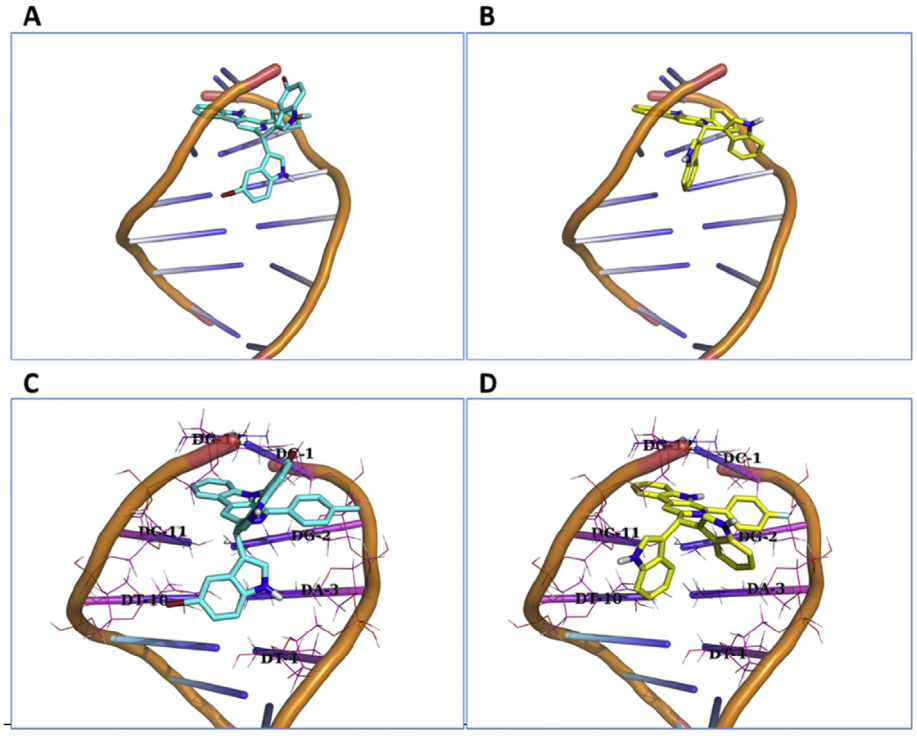

Fig. 12. A) and B) Combilexin type binding mode of compounds **7g** and **7r**, C) and D) Binding pose and hydrophobic interactions of compounds **7g** and **7r** respectively in 44D binding pocket of DNA (PDB ID: 1NAB), compounds **7g** and **7r** were shown in stick and coloured by the atom type. Carbon: Cyan (**7g**), yellow (**7r**); Bromine: red; hydrogen: white; nitrogen: blue; fluorine: ice blue). (For interpretation of the references to colour in this figure legend, the reader is referred to the web version of this article.)

interactions with dA-3, dT-4 and dT-10 nucleotides present in the groove with the help of Sp3 carbon present in bis-indole motif (Fig. 12C and D). In addition, dG-12 present in groove also showing interaction with C-3 Substituent of compound **7g**.

The molecular docking studies revealed that the β-carboline ring is responsible for intercalation and C-1 substituent especially in **7g** come close to dG-2, dA-3 of DNA and show effective interaction. Further, the C-3 substituent was responsible for interaction with nucleotides present at the groove in 44D binding pocket of 1NAB. Hence, these compounds have enough structural features to show the combilexin type of binding even though smaller in molecular size along with Topoisomerase I Inhibitor properties.

3. Conclusion

In conclusion, a new series of β-carboline-bisindole compounds of varying substitutions at C-1 and C-3 positions were synthesized involving two pharmacophores and their antiproliferative properties were evaluated against various human cancer cell lines. All the compounds exhibited pronounced antiproliferative activity against prostate cancer cell line. Among them **7g** and **7r** compounds were found to possess significant cytotoxicity. Further assays such as Annexin V-FITC assay revealed that these compounds induce apoptosis. Cell cycle histograms indicate that these compounds stop the cell cycle at G2/M phase. In addition, these compounds inhibit topoisomerase I by binding with DNA-topoisomerase complex and can also cleave the pBR322 plasmid upon irradiation with UV light. DNA binding assays and molecular docking studies support that these compounds abide by combilexin type interactions with DNA.

4. Experimental section

4.1. Chemistry

All solvents and reagents were purchased from the commercial sources and were used without further purification. Reactions were monitored by TLC on silica gel glass plate containing 60 GF-254, and visualization was done by UV light and iodine vapor. ^{1}H and ^{13}C NMR spectra were recorded on Bruker UXNMR/XWIN-NMR (300 MHz) or InovaVarian-VXR-unity (400, 500 MHz) instruments. Chemical shifts were expressed in parts per million (δ in ppm) downfield from TMS expressed as internal standard and coupling constants are expressed in Hz. ^{1}H NMR spectral data were reported in the following order: multiplicity (s, singlet; brs, broad singlet; d, doublet; dd, doublet of doublets; t, triplet; m, multiplet), coupling constants in Hz, and number of protons. ESI mass spectra were recorded on a Micromass Quattro LC using ESI + software with capillary voltage 3.98 kV and an ESI mode positive ion trap detector. High resolution mass spectra were recorded on a QSTAR XL Hybrid MS-MS mass spectrometer. Melting points were determined with an electro thermal digital melting point apparatus IA9100 and are uncorrected. The purity of tested compounds was P98% as determined by HPLC performed on a Shimadzu LC-20AD apparatus equipped with a SPD-M20A diode array detector and a Shimadzu SIL- 20AC auto injector using C18 column (waters 5 μM C18, 4.6 mm 250 mm column). Elution conditions: mobile phase A (85%)- acetonitrile; mobile phase B(15%)-water, P^H 4.3 adjusted with 0.1% formic acid + 10 mmol NH_4OAc. The flow rate was 1.0 mL/min and the injection volume was 5 μL at 25 °C and detection at 254 nm.

4.1.1. General procedure for the preparation of compounds (**3a-d**)

To a stirred solution of L-tryptophan (**1**, 0.1 mol) in methanol (40 ml) was added (0.11 mol) thionly chloride drop wise at 0 °C and the reaction mixture was stirred for 8 h at 27 °C then, excess solvent was removed under vacuum and the crude product was co-distilled with toluene (2 × 15 mL) to obtain a solid. The resulted solid was extracted with DCM (3 × 40 mL), washed with saturated $NaHCO_3$ solution, the combined organic layers were dried over anhydrous Na_2SO_4 and evaporated under vacuum to obtain white solid tryptophan ester (**2**). To a solution mixture of tryptophan ester (0.023 mol) and substituted benzaldehyde (0.023 mol) in toluene (50 mL), a catalytic amount of *p*-TSA was added and the reaction mixture was refluxed at 110 °C for 12 h. After completion of the reaction, the solvent was removed under the vacuum, the crude mixture was extracted with ethyl acetate. The organic layers were dried over anhydrous Na_2SO_4 and concentrated under vacuum. The resulted diasteriomeric mixture (**3a-d**) was directly used for the next step without any further purification.

4.1.2. General procedure for the synthesis of methyl-1-phenyl-9H-pyrido[3,4-b]indole-3-carboxylates (**4a-d**)

To a stirred solution of compounds **3a-d** (0.01 mol) in DMF was added triethylamine (0.03 mol) and trichloroisocyanuric acid (0.012 mol) solution in DMF drop wise at −20 °C. The reaction mixture was slowly warmed to 0 °C and stirred for 2 h, after completion of the reaction, was monitored by TLC, added ice water, filtered the resulted precipitate and dried under the vacuum to obtain the product (**4a-d**). These products were directly used for the next step without any further purification.

4.1.3. General procedure for the synthesis of (1-phenyl-9H-pyrido [3,4-b]indol-3-yl)methanol (**6a-d**)

To the compound **4a-d** (0.019 mol) taken in dry THF (60 ml) was added $LiAlH_4$ (0.076 mol) portion wise at −5 to 0 °C and continued stirring for 4 h at 27 °C, after completion of the reaction excess of $LiAlH_4$ was quenched by adding $Na_2SO_4{\cdot}10H_2O$ until the bubbling stops, filtered through celite and concentrated under vacuum. To the crude product **5a-d** (0.014 mol) in dry CH_2Cl_2 was added DMP (0.021 mol) and stirred for 2 h at 27 °C. After completion of the reaction, the reaction mixture was washed with water (2 × 50 ml), the organic layers were dried over Na_2SO_4 and concentrated under vacuum. The resulted crude products was purified by column chromatography (ethyl acetate: hexane) to afford the compounds (**6a-d**) with high purity.

*4.1.3.1. 1-(3,4,5-Trimethoxyphenyl)-9H-pyrido[3,4-b]indole-3-carbaldehyde (**6a**).* Yellow solid: 81% yield; mp: 220–224 °C; ^{1}H NMR (300 MHz, CDCl3 + DMSO-d_6) δ (ppm): 10.21 (s, 1H), 9.2 (bs, 1H), 8.71 (s, 1H), 8.23 (d, J = 7.9 Hz, 1H), 7.64–7.63 (m, 2H), 7.42–7.39 (m, 1H), 7.13 (s, 2H), 3.92 (s, 9H); MS (ESI): m/z 363 [M + H]$^+$.

*4.1.3.2. 1-(4-Methylphenyl)-9H-pyrido[3,4-b]indole-3-carbaldehyde (**6b**).* White solid of 79% yield; mp: 189–190 °C; ^{1}H NMR (300 MHz, DMSO-d_6) δ (ppm): 11.4 (bs, 1H), 10.25 (s, 1H), 8.69 (s, 1H), 8.22 (d, J = 7.9 Hz, 1H), 8.13 (t, J = 8.4 Hz, 3H), 7.7 (d, J = 7.7 Hz, 1H), 7.6 (t, J = 7.3 Hz, 2H), 7.5 (s, 1H), 2.28 (s, 3H); MS (ESI): m/z 287 [M + H]$^+$.

*4.1.3.3. 1-(4-Methoxyphenyl)-9H-pyrido[3,4-b]indole-3-carbaldehyde (**6c**).* Pale yellow solid: 82% yield; mp: 213–217 °C; ^{1}H NMR (300 MHz, CDCl3 + DMSO-d_6) δ (ppm): 10.3 (s, 1H), 8.9 (s, 1H), 8.7 (s, 1H), 8.2 (d, J = 7.94 Hz, 1H), 7.62 (m, 3H), 7.37 (m, 2H), 7.14 (m, 2H), 3.87 (s, 3H); MS (ESI): m/z 303 [M + H]$^+$.

*4.1.3.4. 1-(4-Fluorophenyl)-9H-pyrido[3,4-b]indole-3-carbaldehyde (**6d**).* White solid of 85% yield; mp: 189–190 °C; ^{1}H NMR (300 MHz, DMSO-d_6) δ (ppm): 11.42 (bs, 1H), 10.25 (s, 1H), 8.69 (s, 1H), 8.22 (d, J = 7.9 Hz, 1H), 8.13 (t, J = 8.4 Hz, 3H), 7.7 (d, J = 7.7 Hz, 1H), 7.6 (t, J = 7.3 Hz, 2H), 7.5 (s, 1H); MS (ESI): m/z 291 [M + H]$^+$.

4.1.4. General procedure for the synthesis β-carboline-bisindole compounds (**7a-7ab**)

To a solution of β-carboline aldehyde (1 equiv.) in water-ethanol (3:1) was added respective substituted indole (2 equiv.) and 2 mol % of catalyst Amberlite IR-120H. The reaction mixture was stirred for 6 h at 80 °C, after completion of the reaction, monitored by the TLC and the appearance of solid is also an indication of the product formation. Then the reaction mixture was cooled to room temperature and filtered the resulted solid. The crude products were purified by the filter column chromatography to afford the pure respective β-carboline-bisindole compounds in good to excellent yields.

*4.1.4.1. 3-(bis(5-bromo-1H-indol-3yl)methyl)-1-(3,4,5-trimethoxyphenyl)-9H-pyrido[3,4-b]indole (**7a**).* Brown solid; yield 86%; mp: 194–196 °C; ^{1}H NMR (300 MHz, $CDCl_3$+DMSO-d_6) δ 11.15 (s, 1H), 10.57 (s, 2H), 7.99 (d, J = 7.8 Hz, 1H), 7.87 (s, 1H), 7.73 (s, 1H), 7.57 (d, J = 12.3 Hz, 3H), 7.48 (d, J = 7.6 Hz, 1H), 7.30–7.23 (m, 3H), 7.14 (t, J = 8.9 Hz, 3H), 6.92 (s, 2H), 6.16 (s, 1H), 3.96 (s, 6H), 3.88 (s, 3H); ^{13}C NMR (75 MHz, DMSO-d_6) δ 152.77, 141.51, 140.55, 137.61, 135.11, 131.68, 128.38, 127.64, 124.81, 123.21, 121.38, 120.94, 120.73, 118.89, 117.40, 112.69,111.97, 111.67, 110.99, 105.54, 60.15, 55.64, 41.92; HRMS (ESI): calcd for $C_{37}H_{29}N_4O_3Br_2$ [M+H]$^+$ 735.0601, found 735.0597.

*4.1.4.2. 3-(di(1H-indol-3-yl)methyl)-1-(3,4,5-trimethoxyphenyl)-9H-pyrido[3,4-b]indole (**7b**).* Light brown solid; yield 91%; mp: 186–188 °C; ^{1}H NMR (300 MHz, $CDCl_3$+DMSO-d_6) δ 11.21 (s, 1H), 10.49 (s, 2H), 7.99 (d, J = 7.8 Hz, 1H), 7.93 (s, 2H), 7.59 (d, J = 8.1 Hz,

1H), 7.46 (d, $J = 7.7$ Hz, 3H), 7.35 (d, $J = 8.1$ Hz, 2H), 7.15 (t, $J = 7.5$ Hz, 1H), 7.03 (t, $J = 7.5$ Hz, 3H), 6.97 (s, 2H), 6.87 (t, $J = 7.4$ Hz, 2H), 6.22 (s, 1H), 3.94 (s, 6H), 3.85 (s, 3H); ^{13}C NMR (75 MHz, DMSO-d_6) δ 153.03, 136.57, 131.65, 128.03, 126.90, 123.67, 121.50, 120.80, 119.25, 118.15, 112.38, 111.40, 105.98, 60.17, 55.88, 42.28; HRMS (ESI): calcd for $C_{37}H_{31}N_4O_3$ $[M+H]^+$ 579.2391, found 579.2388.

*4.1.4.3. 3-(bis(2-methyl-5-nitro-1H-indol-3-yl)methyl)-1-(3,4,5-trimethoxyphenyl)-9H-pyrido[3,4-b]indole (**7c**).* Light green solid; yield 85%; mp: 213–215 °C; ^{1}H NMR (300 MHz, $CDCl_3$+DMSO-d_6) δ 11.01 (s, 1H), 10.85 (s, 2H), 7.90 (dd, $J = 10.4$, 8.3 Hz, 3H), 7.72 (s, 2H), 7.46 (s, 3H), 7.34 (d, $J = 9.0$ Hz, 2H), 7.05 (s, 2H), 6.89 (s, 1H), 6.40 (s, 1H), 3.86 (d, $J = 9.8$ Hz, 3H), 3.78 (s, 6H), 2.21 (s, 6H); ^{13}C NMR (75 MHz, DMSO-d_6) δ 152.04, 151.74, 141.39, 140.59, 140.23, 138.98, 137.40, 135.23, 130.92, 126.68, 126.45, 120.12, 119.86, 117.98, 114.71, 114.01, 111.19, 109.16, 104.92, 104.55, 59.02, 54.78, 54.35, 40.06, 11.03; HRMS (ESI): calcd for $C_{39}H_{33}N_6O_7$ $[M+H]^+$ 697.2405, found 697.2403.

*4.1.4.4. 3-(bis(5-nitro-1H-indol-3-yl)methyl)-1-(3,4,5-trimethoxyphenyl)-9H-pyrido[3,4-b]indole (**7d**).* Light yellow solid; yield 81%; mp: 346–348 °C; ^{1}H NMR (300 MHz, $CDCl_3$+DMSO-d_6) δ 11.28 (s, 2H), 11.22 (s, 1H), 8.41 (d, $J = 7.9$ Hz, 1H), 8.02–7.92 (m, 4H), 7.77 (s, 1H), 7.60 (d, $J = 8.2$ Hz, 1H), 7.47 (t, $J = 7.2$ Hz, 3H), 7.25 (s, 2H),7.16 (d, $J = 8.4$ Hz, 3H), 6.37 (s, 1H), 3.95 (s, 6H), 3.87 (s, 3H); ^{13}C NMR (75 MHz, $CDCl_3$+DMSO-d_6) δ 152.80, 150.70, 141.45, 141.14, 140.19, 139.73, 137.61, 133.89, 131.88, 130.23, 127.59, 126.74, 125.93,120.89, 120.75, 120.30, 118.88, 116.43, 116.27,112.02, 111.76, 111.23, 105.52, 60.15, 55.58, 42.16; HRMS (ESI): calcd for $C_{37}H_{29}N_6O_7$ $[M+H]^+$ 669.2092, found 669.2099.

*4.1.4.5. 3,3'-((1-(3,4,5-trimethoxyphenyl)-9H-pyrido[3,4-b]indol-3-yl)methelene)bis(1H-indole-5-carbonitrile) (**7e**).* White solid; yield 80%; mp: 195–197 °C; ^{1}H NMR (300 MHz, $CDCl_3$+DMSO-d_6) δ 10.97 (s, 1H), 10.85 (s, 2H), 7.97 (d, $J = 7.8$ Hz, 1H), 7.83 (s, 1H), 7.78 (s, 1H), 7.61 (d, $J = 8.2$ Hz, 1H), 7.49 (dd, $J = 12.9$, 8.3 Hz, 4H), 7.32 (d, $J = 8.4$ Hz, 2H), 7.21–7.15 (m, 3H), 6.99 (s, 2H), 6.29 (s, 1H), 3.95 (s, 6H), 3.89 (s, 3H); ^{13}C NMR (75 MHz, $CDCl_3$+DMSO-d_6) δ 152.89, 150.88, 141.37, 141.21, 138.34, 137.64, 133.95, 131.93, 130.30, 127.61, 126.45, 125.74, 124.91, 123.54, 120.94, 120.69, 118.92, 118.78, 112.06, 111.76, 105.47, 100.65, 60.31, 55.67, 42.19; HRMS (ESI): calcd for $C_{39}H_{29}N_6O_3$ $[M+H]^+$ 629.2296, found 629.2297.

*4.1.4.6. 3-(di(1H-indol-3-yl)methyl)-1-(p-tolyl)-9H-pyrido[3,4-b]indole (**7f**).* Brown solid; yield 88%; mp: 323–325 °C; ^{1}H NMR (300 MHz, $CDCl_3$+DMSO-d_6) δ 11.24 (s,1H), 10.62 (s, 2H), δ 8.01 (dd, $J = 22.2$, 9.9 Hz, 4H), 7.69 (d, $J = 3.0$ Hz, 1H), 7.61–7.58 (m, 2H), 7.45 (d, $J = 7.7$ Hz, 2H), 7.37 (dd, $J = 12.5$, 8.0 Hz, 4H), 7.15 (t, $J = 7.1$ Hz, 1H), 7.02 (t, $J = 7.6$ Hz, 2H), 6.94 (s, 1H), 6.87 (t, $J = 7.5$ Hz, 2H), 6.22 (s, 1H), 2.46 (s, 1H); ^{13}C NMR (75 MHz, $CDCl_3$+DMSO-d_6) δ 150.92, 141.55, 140.31, 139.86, 137.78, 135.71, 131.98, 130.30, 129.09, 128.39, 127.69, 126.86, 126.03, 120.96, 120.43, 119.05, 116.83, 116.40, 112.18, 111.64, 111.41, 42.56, 21.02; HRMS (ESI): calcd for $C_{35}H_{27}N_4$ $[M+H]^+$ 503.2230, found 503.2218.

*4.1.4.7. 3-(bis(5-bromo-1H-indol-3-yl)methyl)-1-(p-tolyl)-9H-pyrido[3,4-b]indole (**7g**).* Brown solid; yield 84%; mp: 186–188 °C; ^{1}H NMR (300 MHz, $CDCl_3$+DMSO-d_6) δ 10.74 (s, 1H), 10.37 (s, 2H), 7.96 (d, $J = 7.7$ Hz, 3H), 7.83 (s, 1H), 7.61 (s, 3H), 7.46 (t, $J = 7.6$ Hz, 1H), 7.38 (d, $J = 7.7$ Hz, 2H), 7.27 (d, $J = 8.6$ Hz, 2H), 7.15 (dd, $J = 14.4$, 7.5 Hz, 3H), 6.91 (s, 2H), 6.13 (s, 1H), 2.45 (s, 3H); ^{13}C NMR (75 MHz, DMSO-d_6) δ 151.98, 141.86, 141.09, 138.23, 135.41, 131.81, 130.56, 129.54, 128.76, 128.56, 128.30, 125.28, 123.53, 121.96, 121.60, 121.02, 119.55, 117.70, 113.61, 112.58, 112.05, 111.11, 42.38, 21.19; HRMS (ESI): calcd for $C_{35}H_{25}N_4Br_2$ $[M+H]^+$ 659.0440, found 659.0442; HPLC:t_R 5.63min, purity 97.4%.

*4.1.4.8. 3-(bis(2-methyl-5-nitro-1H-indol-3-yl)methyl)-1-(p-tolyl)-9H-pyrido[3,4-b]indole (**7h**).* Yellow solid; yield 81%; mp: 238–240 °C; ^{1}H NMR (300 MHz, $CDCl_3$+DMSO-d_6) δ 11.24 (s, 2H), 11.16 (d, $J = 7.1$ Hz, 1H), 8.08–7.95 (m, 2H), 7.85–7.80 (m, 6H), 7.61 (t, $J = 7.8$ Hz, 1H), 7.49–7.39 (m, 2H), 7.32 (d, $J = 9.5$ Hz, 2H), 7.27 (d, $J = 8.1$ Hz, 1H), 7.16 (t, $J = 7.4$ Hz, 1H), 6.30 (s, 1H), 2.19 (s, 3H), 2.14 (s, 6H); ^{13}C NMR (75 MHz, DMSO-d_6) δ 149.93, 141.52, 139.95, 138.40, 137.60, 135.96, 131.96, 130.02, 129.95, 128.87, 128.26, 127.59, 121.03, 120.90, 118.94, 115.90, 115.14, 114.97, 112.18, 111.96, 110.13, 41.50, 20.89, 12.04; HRMS (ESI): calcd for $C_{37}H_{29}N_6O_4$ $[M+H]^+$ 621.2245, found 621.2249.

*4.1.4.9. 3-(bis(5-nitro-1H-indol-3-yl)methyl)-1-(p-tolyl)-9H-pyrido[3,4-b]indole (**7i**).* Yellow solid; yield 78%; mp: 242–244 °C; ^{1}H NMR (300 MHz, $CDCl_3$+DMSO-d_6) δ 11.28 (s, 2H), 11.05 (s, 1H), 8.49 (d, $J = 1.8$ Hz, 2H), 8.03–7.94 (m, 6H), 7.80 (d, $J = 5.0$ Hz, 1H), 7.60 (d, $J = 8.2$ Hz, 1H), 7.44 (d, $J = 9.0$ Hz, 3H), 7.36 (d, $J = 7.9$ Hz, 2H), 7.23 (s, 1H), 7.17 (t, $J = 7.5$ Hz, 1H), 6.32 (s, 1H), 2.45 (s, 3H); ^{13}C NMR (75 MHz, $CDCl_3$+DMSO-d_6) δ 150.74, 141.37, 140.13, 139.68, 137.60, 135.53, 131.80, 130.11, 128.91, 128.20, 127.51, 126.67, 125.85, 120.77, 120.24, 118.86, 116.64, 116.21, 112.00, 111.46, 111.22, 42.37, 20.83; HRMS (ESI): calcd for $C_{35}H_{25}N_6O_4$ $[M+H]^+$ 593.1932, found 593.1932.

*4.1.4.10. 3,3'-((1-(p-tolyl)-9H-pyrido[3,4-b]indol-3-yl)methylene) bis(1H-indole-5-carbonitrile) (**7j**).* White solid; yield 79%; mp: 254–256 °C; ^{1}H NMR (300 MHz, DMSO-d_6) δ 11.15 (d, $J = 7.6$ Hz, 3H), 7.96 (dd, $J = 19.5$, 11.7 Hz, 6H), 7.61 (d, $J = 8.1$ Hz, 1H), 7.47 (d, $J = 8.3$ Hz, 3H), 7.39 (d, $J = 7.4$ Hz, 2H), 7.29 (d, $J = 8.1$ Hz, 2H), 7.17 (s, 3H), 6.21 (s, 1H), 2.46 (s, 3H). ^{13}C NMR (75 MHz, $CDCl_3$+DMSO-d_6) δ 150.94, 141.38, 138.23, 137.59, 131.71, 128.97, 128.15, 127.50, 126.35, 125.69, 125.02, 123.26, 120.86, 120.78, 120.53, 118.86, 118.64, 112.26, 112.04, 111.40, 100.37, 42.35, 20.85; HRMS (ESI): calcd for $C_{37}H_{25}N_6$ $[M+H]^+$ 553.2135, found 553.2133.

*4.1.4.11. 3-(di(1H-indol-3-yl)methyl)-1-(4-methoxyphenyl)-9H-pyrido[3,4-b]indole (**7k**).* Brown solid; yield 84%; mp: 212–214 °C; ^{1}H NMR (300 MHz, DMSO-d_6) δ 11.06 (s, 1H), 10.46 (s, 2H), 8.04 (d, $J = 8.5$ Hz, 2H), 7.96 (d, $J = 8.3$ Hz, 1H), 7.86 (d, $J = 4.1$ Hz, 1H), 7.58 (d, $J = 8.0$ Hz, 1H), 7.45 (d, $J = 5.6$ Hz, 3H), 7.34 (d, $J = 8.0$ Hz, 2H), 7.06 (dt, $J = 23.4$, 7.6 Hz, 5H), 6.88 (dd, $J = 15.6$, 7.8 Hz, 4H), 6.19 (s, 1H), 3.88 (d, $J = 2.4$ Hz, 3H); ^{13}C NMR (75 MHz, $CDCl_3$+DMSO-d_6) δ 159.25, 152.48, 141.30, 140.50, 136.38, 131.35, 129.85, 129.51, 127.27, 126.72, 123.31, 120.84, 120.49, 119.04,118.68, 118.13, 117.83, 113.57, 111.92, 110.96, 54.87, 42.53; HRMS (ESI): calcd for $C_{35}H_{27}N_4O$ $[M+H]^+$ 519.2179, found 519.2167.

*4.1.4.12. 3-(bis(2-methyl-5-nitro-1H-indol-3-yl)methyl)-1-(4-methoxyphenyl)-9H-pyrido[3,4-b]indole (**7l**).* Yellow solid; yield 83%; mp: 239–241 °C; ^{1}H NMR (300 MHz, $CDCl_3$+DMSO-d_6) δ 11.39 (s, 3H), 8.02–7.94 (m, 3H), 7.90 (s, 1H), 7.82 (d, $J = 7.1$ Hz, 4H), 7.63 (d, $J = 8.2$ Hz, 1H), 7.49 (t, $J = 7.6$ Hz, 1H), 7.34 (d, $J = 9.5$ Hz, 2H), 7.19 (t, $J = 8.6$ Hz, 3H), 6.30 (s, 1H), 3.33 (s, 3H), 2.20 (s, 6H); ^{13}C NMR (75 MHz, DMSO-d_6) δ 160.59, 150.03, 141.64, 140.25, 139.91, 138.41, 136.07, 134.61, 131.86, 130.37, 130.27, 128.53, 127.89, 127.46, 121.23, 119.17, 115.93, 115.16, 114.96, 112.25, 110.33, 63.43, 41.40, 12.04; HRMS (ESI): calcd for $C_{37}H_{29}N_6O_5$ $[M+H]^+$ 637.2194, found 637.2191.

*4.1.4.13. 3-(bis(5-bromo-1H-indol-3-yl)methyl)-1-(4-methoxyphenyl)-9H-pyrido[3,4-b]indole (**7m**).* Brown solid; yield 81%; mp: 168–170 °C; ^{1}H NMR (300 MHz, $CDCl_3$+DMSO-d_6) δ 11.05 (s, 1H), 10.66 (s, 2H), 8.02 (t, $J = 9.1$ Hz, 2H), 7.86 (s, 2H), 7.60 (d,

J = 9.4 Hz, 3H), 7.46 (t, J = 7.4 Hz, 1H), 7.28 (d, J = 8.6 Hz, 2H), 7.14 (dd, J = 20.6, 7.9 Hz, 5H), 6.99 (s, 2H), 6.09 (s, 1H), 3.90 (s, 3H); ^{13}C NMR (75 MHz, $CDCl_3$+DMSO-d_6) δ 159.34, 151.54, 141.38, 135.08, 131.40, 129.97, 129.57, 128.35, 127.46, 124.74, 123.11, 121.53, 120.86, 120.76, 118.83, 117.39, 113.70, 112.83, 112.02, 110.83, 54.90, 42.34; HRMS (ESI): calcd for $C_{35}H_{25}N_4OBr_2$ $[M+H]^+$ 675.0390, found 675.0392.

*4.1.4.14. 3-(bis(5-nitro-1H-indol-3-yl)methyl)-1-(4-methoxyphenyl)-9H-pyrido[3,4-b]indole (**7n**).* Yellow solid; yield 79%; mp: 299–301 °C; ^{1}H NMR (500 MHz, $CDCl_3$) δ 11.29 (s, 2H), 11.06 (s, 1H), 8.50 (d, J = 2.0 Hz, 2H), 8.03 (dd, J = 11.8, 4.9 Hz, 3H), 7.97–7.92 (m, 3H), 7.83 (d, J = 2.0 Hz, 1H), 7.60 (s, 1H), 7.45 (t, J = 7.5 Hz, 3H), 7.24 (s, 1H), 7.17 (d, J = 7.4 Hz, 1H), 7.08 (d, J = 8.6 Hz, 2H), 6.31 (s, 1H), 3.89 (s, 3H); ^{13}C NMR (75 MHz, DMSO-d_6) δ 159.36, 150.65, 141.35, 140.12, 139.69, 131.64, 130.82, 130.08, 129.59, 129.58, 127.49, 126.66, 125.84, 120.82, 120.23, 118.86, 116.66, 116.23, 113.64, 111.98, 111.20, 54.89, 42.35; HRMS (ESI): calcd for $C_{35}H_{25}N_6O_5$ $[M+H]^+$ 609.1881, found 609.1876.

*4.1.4.15. 3,3'-((1-(4-methoxyphenyl)-9H-pyrido[3,4-b]indol-3-yl) methelene)bis(1H-indole-5-carbonitrile) (**7o**).* Brown solid; yield 77%; mp: 238–240 °C; ^{1}H NMR (300 MHz, $CDCl_3$+DMSO-d_6) δ 11.36 (d, J = 7.6 Hz, 3H), 8.06 (dd, J = 23.1, 8.6 Hz, 6H), 7.62 (d, J = 8.1 Hz, 1H), 7.50 (d, J = 8.3 Hz, 3H), 7.32 (d, J = 7.1 Hz, 4H), 7.23–7.09 (m, 3H), 6.24 (s, 1H), 3.89 (s, 3H); ^{13}C NMR (75 MHz, DMSO-d_6) δ 159.49, 151.11, 141.52, 141.04, 138.24, 131.47, 129.61, 126.47, 125.93, 125.26, 123.33, 121.17, 120.67, 119.07, 118.79, 113.96, 112.56, 112.27, 100.30, 55.09, 42.14; HRMS (ESI): calcd for $C_{37}H_{25}N_6O$ $[M+H]^+$ 569.2084, found 569.2077.

*4.1.4.16. 3-(bis(5-fluoro-1H-indol-3-yl)methyl)-1-(4-methoxyphenyl)-9H-pyrido[3,4-b]indole (**7p**).* Light brown solid; yield 80%; mp: 210–212 °C; ^{1}H NMR (300 MHz, $CDCl_3$+DMSO-d_6) δ 11.30 (s, 1H), 10.67 (s, 2H), 8.04 (d, J = 38.6 Hz, 3H), 7.64 (d, J = 25.3 Hz, 2H), 7.45–7.37 (m, 6H), 7.14 (s, 1H), 6.98 (d, J = 17.7 Hz, 4H), 6.88 (s, 1H), 6.21 (s, 1H), 4.29 (s, 1H); ^{13}C NMR (75 MHz, $CDCl_3$+DMSO-d_6) δ 160.59, 160.08, 157.51, (d, J = 234.3 Hz), 148.73, 148.18, 141.27, 140.67, 135.35, 129.60, 129.10, 128.79, 127.56, 125.33, 122.14, 120.67, 119.98, 117.18, 115.05, 114.55, 112.00, 111.65, 111.53, 110.05, 105.12, 104.81, 104.32, 55.58, 42.92; HRMS (ESI): calcd for $C_{35}H_{25}N_4OF_2$ $[M+H]^+$ 555.1991, found 555.1983.

*4.1.4.17. 3-(bis(5-methoxy-1H-indol-3-yl)methyl)-1-(4-methoxyphenyl)-9H-pyrido[3,4-b]indole (**7q**).* White solid; yield 85%; mp: 191–193 °C; ^{1}H NMR (500 MHz, $CDCl_3$) δ 8.39 (s, 1H), 7.94 (d, J = 7.9 Hz, 1H), 7.86 (d, J = 8.5 Hz, 2H), 7.82 (s, 1H), 7.47–7.41 (m, 2H), 7.17 (dd, J = 10.7, 8.5 Hz, 3H), 7.01 (d, J = 8.3 Hz, 2H), 6.94 (d, J = 2.3 Hz, 1H), 6.79 (s, 1H), 6.77 (s, 1H), 6.76 (s, 2H), 6.24 (s, 1H), 3.83 (s, 3H), 3.62 (s, 6H); ^{13}C NMR (101 MHz, $CDCl_3$) δ 160.01 (s), 153.70, 153.54, 141.75, 140.92, 132.19, 132.06, 131.46, 130.80, 129.66, 128.25, 127.89, 124.60, 122.24, 122.04, 119.93, 119.27, 114.56, 112.17, 111.92, 111.79, 111.59, 102.27, 55.96, 55.49, 43.24; HRMS (ESI): calcd for $C_{37}H_{31}N_4O_3$ $[M+H]^+$ 579.2391, found 579.2380.

*4.1.4.18. 3-(di(1H-indol-3-yl)methyl)-1-(4-fluorophenyl)-9H-pyrido[3,4-b]indole (**7r**).* Light brown solid; yield 82%; mp: 195–197 °C; ^{1}H NMR (300 MHz, $CDCl_3$+DMSO-d_6) δ 11.06 (s, 1H), 10.30 (d, J = 22.1 Hz, 2H), 8.09 (s, 1H), 7.97 (d, J = 7.4 Hz, 1H), 7.91 (s, 1H), 7.76–7.68 (m, 1H), 7.59 (d, J = 8.1 Hz, 1H), 7.46 (t, J = 9.7 Hz, 3H), 7.36 (d, J = 8.1 Hz, 1H), 7.29 (d, J = 4.8 Hz, 2H), 7.16 (t, J = 7.3 Hz, 1H), 7.05 (dd, J = 13.7, 6.2 Hz, 2H), 6.89 (t, J = 7.1 Hz, 5H), 6.28 (s, 1H); ^{13}C NMR (75 MHz, $CDCl_3$+DMSO-d_6) δ 161.49 (d, J = 247.1 Hz), 151.88, 140.76, 138.86, 135.74, 130.86, 129.55 (d, J = 7.4 Hz), 128.76, 126.86, 126.03, 125.70, 125.32, 122.70, 121.04, 120.24, 119.88, 118.37, 118.17, 117.36, 117.20, 114.32 (d, J = 21.0 Hz), 111.22, 110.90, 110.30, 41.79; HRMS (ESI): calcd for $C_{34}H_{24}N_4F$ $[M+H]^+$ 507.1979, found 507.1970; HPLC:t_R 4.87 min, purity 96.9%.

*4.1.4.19. 3-(bis(2-methyl-5-nitro-1H-indol-3-yl)methyl)-1-(4-fluorophenyl)-9H-pyrido[3,4-b]indole (**7s**).* Yellow solid; yield 80%; mp: 241–243 °C; ^{1}H NMR (300 MHz, DMSO-d_6) δ 10.67 (s, 2H), 10.54 (s, 1H), 7.92 (dt, J = 13.0, 7.5 Hz, 5H), 7.83 (s, 1H), 7.75 (s, 1H), 7.60 (d, J = 8.1 Hz, 1H), 7.49 (t, J = 7.6 Hz, 1H), 7.42 (s, 1H), 7.30 (d, J = 8.9 Hz, 2H), 7.21–7.13 (m, 3H), 6.36 (s, 1H), 2.16 (s, 6H); ^{13}C NMR (75 MHz, $CDCl_3$+DMSO-d_6) δ 162.20 (d, J = 247.5 Hz), 149.92, 141.45, 140.46, 139.95, 138.34, 135.84, 134.49, 131.87, 130.15, (d, J = 8.4 Hz), 127.64, 127.41, 120.95, 120.83, 118.95, 115.77, 115.25, 114.81, 144.67, 112.04 (d, J = 21.3 Hz), 109.94, 41.38, 11.94; HRMS (ESI): calcd for $C_{36}H_{26}N_6O_4F$ $[M+H]^+$ 625.1994, found 625.1997.

*4.1.4.20. 3-(bis(5-nitro-1H-indol-3-yl)methyl)-1-(4-fluorophenyl)-9H-pyrido[3,4-b]indole (**7t**).* Light green solid; yield 77%; mp: 232–234 °C; ^{1}H NMR (300 MHz, $CDCl_3$+DMSO-d_6) δ 11.28 (s, 2H), 11.14 (s, 1H), 8.49 (d, J = 2.1 Hz, 2H), 8.11 (dd, J = 8.7, 5.5 Hz, 2H), 8.03 (d, J = 7.8 Hz, 1H), 7.97 (d, J = 2.4 Hz, 1H), 7.94 (d, J = 2.2 Hz, 1H), 7.80 (s, 1H), 7.60 (d, J = 8.2 Hz, 1H), 7.47 (dd, J = 14.7, 8.1 Hz, 3H), 7.22 (dd, J = 11.8, 10.0 Hz, 5H), 6.33 (s, 1H); ^{13}C NMR (75 MHz, $CDCl_3$+DMSO-d_6) δ 162.19 (d, J = 247.2 Hz), 150.73, 141.46, 140.08, 139.65, 134.46, 131.70, 130.23 (d, J = 8.1 Hz), 127.67, 126.66, 125.78, 120.90, 120.69, 120.09, 118.98, 116.61, 116.18, 115.01 (d, J = 21.3 Hz), 111.97, 111.80, 111.24, 42.29 HRMS (ESI): calcd for $C_{34}H_{22}N_6O_4F$ $[M+H]^+$ 579.1681, found 597.1680; HPLC:t_R 5.53min, purity 98.6%.

*4.1.4.21. 3,3'-((1-(4-fluorophenyl)-9H-pyrido[3,4-b]indol-3-yl)methelene)bis(1H-indole-5-carbonitrile) (**7u**).* Light brown solid; yield 78%; mp: 198–200 °C; ^{1}H NMR (300 MHz, $CDCl_3$+DMSO-d_6) δ 10.91 (s, 3H), 8.07 (s, 2H), 8.00 (d, J = 7.3 Hz, 1H), 7.86 (d, J = 5.9 Hz, 2H), 7.59 (s, 2H), 7.47 (d, J = 8.5 Hz, 3H), 7.31 (d, J = 7.9 Hz, 4H), 7.19 (s, 1H), 7.04 (s, 2H), 6.24 (s, 1H); ^{13}C NMR (75 MHz, $CDCl_3$+DMSO-d_6) δ 162.21 (d, J = 247.8 Hz), 150.88, 141.48, 140.05, 138.26, 134.50, 131.68, 130.19 (d, J = 7.9 Hz), 127.69, 126.29, 125.68, 124.98, 123.30, 120.93, 120.71, 120.53, 118.99, 118.47, 115.10 (d, J = 21.4 Hz), 112.23, 111.98, 111.71, 100.39, 42.27; HRMS (ESI): calcd for $C_{36}H_{22}N_6F$ $[M+H]^+$ 557.1884, found 557.1879.

*4.1.4.22. 3-(bis(5-bromo-1H-indol-3-yl)methyl)-1-(4-fluorophenyl)-9H-pyrido[3,4-b]indole (**7v**).* Light brown solid; yield 79%; mp: 194–196 °C; ^{1}H NMR (500 MHz, $CDCl_3$) δ 8.41 (s, 1H), 8.07 (s, 1H), 7.99 (d, J = 7.9 Hz, 1H), 7.91 (dd, J = 8.5, 5.4 Hz, 2H), 7.83 (s, 1H), 7.63 (s, 1H), 7.52–7.46 (m, 2H), 7.22–7.15 (m, 6H), 6.78 (d, J = 1.6 Hz, 2H), 6.17 (s, 1H); ^{13}C NMR (75 MHz, DMSO-d_6) δ 162.45 (d, J = 247.03 Hz), 151.96, 141.67, 140.15, 135.39, 134.77, 131.89, 130.53, 129.50 (d, J = 8.8 Hz), 127.92, 125.04, 123.48, 121.75, 121.18, 121.01, 119.23, 117.63, 115.41 (d, J = 21.45 Hz), 113.12, 112.25, 111.84, 111.19, 42.60; HRMS (ESI): calcd for $C_{34}H_{22}N_4Br_2F$ $[M+H]^+$ 663.0190, found 663.0197.

*4.1.4.23. 3-(bis(5-fluoro-1H-indol-3-yl)methyl)-1-(4-fluorophenyl)-9H-pyrido[3,4-b]indole (**7w**).* White solid; yield 76%; mp: 164–166 °C; ^{1}H NMR (400 MHz, $CDCl_3$) δ 8.46 (s, 1H), 8.06 (s, 1H), 7.98 (d, J = 7.8 Hz, 1H), 7.91 (s, 2H), 7.84 (s, 1H), 7.48 (q, J = 8.3 Hz, 2H), 7.21 (s, 3H), 7.10 (d, J = 9.6 Hz, 2H), 6.89–6.84 (m, 4H), 6.18 (s, 1H); ^{13}C NMR (75 MHz, $CDCl_3$+DMSO-d_6) δ 156.38 (d, J = 244.7 Hz), 151.97, 141.46, 139.81, 134.74, 133.07, 131.57, 130.27, 127.60, 126.10 (d, J = 7.8 Hz), 120.93, 118.94, 117.88, 115.04 (d, J = 21.2 Hz), 112.00, 111.84, 111.71, 108.88, 108.53, 103.88, 103.57, 42.57; HRMS (ESI): calcd for $C_{34}H_{22}N_4F_3$ $[M+H]^+$ 543.1791, found 543.1787.

*4.1.4.24. 3-(bis(5-methoxy-1H-indol-3-yl)methyl)-1-(4-fluorophenyl)-9H-pyrido[3,4-b]indole (**7x**).* Brown solid; yield 82%; mp: 178–180 °C; ^{1}H NMR (500 MHz, $CDCl_3$) δ 8.39 (s, 1H), 7.96 (d, *J* = 7.9 Hz, 1H), 7.89 (dd, *J* = 15.9, 4.7 Hz, 4H), 7.50–7.44 (m, 2H), 7.22–7.18 (m, 4H), 6.94 (d, *J* = 2.1 Hz, 2H), 6.80 (d, *J* = 2.1 Hz, 1H), 6.78 (s, 2H), 6.25 (s, 1H), 3.63 (s, 6H); ^{13}C NMR (101 MHz, $CDCl_3$) δ 162.94 (d, *J* = 248.1 Hz), 153.64, 153.55, 140.87, 140.69, 134.80, 132.10, 131.96, 131.05, 130.10 (d, *J* = 8.2 Hz), 128.40, 127.75, 124.44, 122.01, 120.04, 119.08, 116.01 (d, *J* = 21.5 Hz), 112.62, 111.85, 111.68, 111.50, 102.20, 55.87, 43.06; HRMS (ESI): calcd for $C_{36}H_{28}N_4O_2F$ $[M+H]^+$ 567.2191, found 567.2183.

*4.1.4.25. 3-(bis(5-fluoro-1H-indol-3yl)methyl)-1-(3,4,5-trimethoxyphenyl)-9H-pyrido[3,4-b]indole (**7y**).* White solid; yield 84%; mp: 190–192 °C; ^{1}H NMR (300 MHz, $CDCl_3$+DMSO-d_6) δ 11.29 (s, 1H), 10.69 (s, 2H), 7.99 (dd, *J* = 21.7, 5.5 Hz, 2H), 7.60 (d, *J* = 8.2 Hz, 1H), 7.45 (t, *J* = 7.6 Hz, 1H), 7.30 (dd, *J* = 7.6, 4.3 Hz, 2H), 7.25 (s, 2H), 7.17 (d, *J* = 7.5 Hz, 1H), 7.08 (d, *J* = 2.8 Hz, 4H), 6.79 (t, *J* = 8.9 Hz, 2H), 6.10 (s, 1H), 3.93 (s, 6H), 3.84 (s, 3H); ^{13}C NMR (75 MHz, $CDCl_3$+DMSO-d_6) δ 156.25 (d, *J* = 232.8 Hz), 152.75, 151.79, 141.40, 140.61, 137.56, 133.98, 133.00, 131.53, 130.06, 127.46,126.96, 126.84, 125.21, 120.91, 120.76, 118.81, 117.89, 111.50, 108.76, 108.41, 105.53, 103.91, 103.60, 59.96, 55.52, 42.43; HRMS (ESI): calcd for $C_{37}H_{29}N_4O_3F_2$ $[M+H]^+$ 615.2202, found 615.2199.

*4.1.4.26. 3-(bis(5-methoxy-1H-indol-3yl)methyl-1-(3,4,5-trimethoxyphenyl)-9H-pyrido[3,4-b]indole (**7z**).* Brown solid; yield 90%; mp: 194–196 °C; ^{1}H NMR (300 MHz, $CDCl_3$+DMSO-d_6) δ 10.78 (s, 1H), 9.67 (s, 2H), 7.96 (d, *J* = 7.8 Hz, 1H), 7.90 (s, 1H), 7.58 (d, *J* = 8.1 Hz, 1H), 7.52 (s, 1H), 7.45 (t, *J* = 7.6 Hz, 1H), 7.26 (s, 1H), 7.22 (d, *J* = 6.5 Hz, 3H), 7.15 (t, *J* = 7.4 Hz, 1H), 6.91 (dd, *J* = 10.2, 1.8 Hz, 3H), 6.72 (dd, *J* = 8.7, 2.2 Hz, 2H), 6.20 (s, 1H), 3.90 (d, *J* = 11.1 Hz, 9H), 3.62 (s, 6H); ^{13}C NMR (75 MHz, $CDCl_3$+DMSO-d_6) δ 152.81, 152.62, 141.25, 140.62, 137.51, 134.29, 131.68, 130.20, 127.35, 127.23, 124.18, 121.04, 120.95, 118.73, 118.11, 111.74, 111.31, 110.48, 105.50, 101.69, 60.27, 55.62, 55.19, 42.58; HRMS (ESI): calcd for $C_{39}H_{35}N_4O_5$ $[M+H]^+$ 639.2602, found 639.2606.

*4.1.4.27. 3-(bis(5-fluoro-1H-indol-3yl)methyl-1-(p-tolyl)-9H-pyrido[3,4-b]indole (**7aa**).* Light brown solid; yield 83%; mp: 195–197 °C; ^{1}H NMR (400 MHz, $CDCl_3$) δ 8.42 (s, 1H), 7.99–7.95 (m, 2H), 7.81 (s, 2H), 7.48–7.42 (m, 2H), 7.32 (d, *J* = 7.8 Hz, 2H), 7.20–7.17 (m, 2H), 7.10 (dd, *J* = 9.8, 2.2 Hz, 2H), 6.88–6.82 (m, 4H), 6.17 (s, 1H), 2.40 (s, 3H); ^{13}C NMR (75 MHz, $CDCl_3$+DMSO-d_6) δ 156.42(d, *J* = 232.7 Hz), 154.88, 151.83, 141.18, 141.07, 137.50, 135.63, 132.98, 131.68, 130.00, 128.86, 128.12, 127.34, 126.95, 126.82, 125.19, 120.90, 120.81, 118.71, 118.06, 111.75, 111.51, 111.39, 111.27, 108.90, 108.55, 104.01, 103.70, 42.59, 20.79; HRMS (ESI): calcd for $C_{35}H_{25}N_4F_2$ $[M+H]^+$ 539.2042, found 539.2035.

*4.1.4.28. 3-(bis(5-methoxy-1H-indol-3yl)methyl-1-(p-tolyl)-9H-pyrido[3,4-b]indole (**7ab**).* Brown solid; yield 88%; mp: 192–194 °C; ^{1}H NMR (500 MHz, $CDCl_3$) δ 8.46 (s, 1H), 7.96 (d, *J* = 7.9 Hz, 1H), 7.89 (s, 1H), 7.83 (d, *J* = 7.9 Hz, 2H), 7.49–7.44 (m, 2H), 7.32 (d, *J* = 7.6 Hz, 2H), 7.19 (dd, *J* = 17.9, 8.3 Hz, 3H), 6.95 (s, 2H), 6.80 (d, *J* = 2.2 Hz, 2H), 6.78 (d, *J* = 2.4 Hz, 1H), 6.27 (s, 1H), 3.64 (s, 6H), 2.17 (s, 3H); ^{13}C NMR (126 MHz, $CDCl_3$) δ 153.77,153.65, 142.02, 140.89, 138.67, 136.08, 132.33, 132.08, 130.86, 129.93, 128.34, 127.94, 124.57, 122.26,122.11, 119.98, 119.39, 112.47, 112.05, 111.76, 111.55, 102.29, 56.00, 43.23, 21.51; HRMS (ESI): calcd for $C_{37}H_{31}N_4O_2$ $[M+H]^+$ 563.2441, found 563.2434.

4.2. Biology

4.2.1. Antiproliferative activity

The Anti cancer activity of the compounds was determined using MTT assay [40]. 1×10^4 cells/well were seeded in 100μl DMEM/MEM, supplemented with 10% FBS in each well of 96-well microculture plates and incubated for 24 h at 37 °C in a CO_2 incubator. After 24 h of incubation, all the synthesized compounds were added to the cells and incubated for 48 h. After 48 h of drug treatment, 10 μl MTT (3-(4, 5-dimethylthiazol-2-yl)- 2,5-diphenyl tetrazolium bromide) (5 mg/mL) was added to each well and the plates were further incubated for 4 h. Then the supernatant from each well was carefully removed, formazon crystals were dissolved in 100 μl of DMSO and absorbance at 570 nm wavelength was recorded.

4.2.2. Topoisomerase I inhibition

The Topoisomerase I inhibitory activity was measured in a DNA cleavage assay as described previously [41]. The pBR 322 plasmid DNA was purchased from Sigma Aldrich, USA and 0.5 μg of DNA was incubated with 1 unit of Topo I enzyme (Invitrogen) in 1X NEB buffer (50 mM potassium acetate, 20 mM Tris acetate, 10 mM magnesium acetate, 1 mM DTT). Camptothecin (at 20 μM) a well-known topo I inhibitor was used as a positive control. Camptothecin and all the synthetic ligands (**7g, 7r** and **7t)** at 20 μM was added to the Topo I-DNA complex and incubated at 37 °C for 30 min, allowing the formation of ternary enzyme-DNA-ligand complex. Assay carried out at IC_{50} concentration did not show noticeable results. Hence, Topo I inhibition experiments were carried out at higher ligand concentration (at 20 μM). Then the enzyme was inactivated by increasing the temperature to 65 °C. After the incubation, the samples was resolved using 1% agarose gel electrophoresis enables the visualization of cleavage products. The pBR322 DNA sample to which no ligand was added considered as control.

4.2.3. DNA photocleavage assay

This experiment was carried out according to the protocol reported by Toshima and co workers [42]. 0.45 μg of pBR322 plasmid DNA was taken in Tris-HCl buffer (50 mM, pH 7.5) and 20 μM of **7g, 7r** and **7t** compounds was added and the total volume was maintained at 20 μl. DNA photocleavage with **7g, 7r** and **7t** hybrids was relatively less at concentrations closer to its IC_{50}. This may be because **7g, 7r** and **7t** hybrids absorption was low even after interaction with CT -DNA (at wavelength around 365 nm). Due to this reason, higher concentration of **7g, 7r** and **7t** hybrids (20 μM) was taken for photocleavage assay. Similar observation was reported earlier when tetrapyridoacridine ligand interaction with DNA [43]. The DNA samples with testing molecules were taken in TPP tissue culture test plate and irradiated with UV light (8 W, 365 nm, 4 cm distance). The DNA sample irradiated with UV-light (at 365 nm) in the absence of **7g, 7r** and **7t** compounds was considered as control. After irradiation, the samples were collected and mixed with 2 μl of loading dye (50% sucrose and 0.25% bromophenol blue). Then, samples were analysed by gel electrophoresis on a 1% agarose horizontal slab gel containing 0.5 μg/ml ethidium bromide in Tris-EDTA buffer (40 mM Tris, 20 mM acetic acid and 1mM EDTA, pH 8.0) at 10 V Cm^{-1}. Gels were photographed under UV light with the Bio-Rad digital camera and analysed with Gel-Pro software.

4.2.4. Cell cycle analysis

Flow cytometric analysis (FACS) was performed to evaluate the distribution of the cells through the cell-cycle phases. DU-145 cells were treated with compounds **7g** and **7r** at 1 and 2 μM

concentrations for 48 h. Untreated and treated cells were harvested, washed with phosphate-buffered saline (PBS), fixed in ice-cold 70% ethanol, and stained with propidium iodide (Sigma–Aldrich). Cell-cycle analysis was performed by flow cytometry (Becton Dickinson FACS Caliber instrument) [44].

4.2.5. Annexin staining assay for apoptosis

DU-145 (1×10^6) cells were seeded in six-well plates and allowed to grow overnight. The medium was then replaced with complete medium containing compounds **7g** and **7r** at 1 and 2 μM concentrations for 48 h. After 48 h of drug treatment, cells from the supernatant and adherent monolayer cells were harvested by trypsinization, washed with PBS at 5000 rpm. Then the cells were stained with Annexin VFITC and propidium iodide using the Annexin-V-FITC apoptosis detection kit (Sigma aldrich). Then the samples were analyzed by flow cytometry as described earlier [45].

4.2.6. UV–visible spectroscopy

UV–visible absorption spectra were recorded using Perkin Elmer ABI 35 Lambda Spectrophotometer (Waltham, MA, USA) at 25 °C. All the experiments were carried out in polystyrene cuvettes to minimize binding of derivatives to the surface of the cuvettes. 50 μM of β-carboline bisindole compounds stock solution was prepared in DMSO and 25.0 μM of CT-DNA in 100 mM *Tris*-HCl (pH 7.0). About 1 ml of 25.0 μM β-carboline bisindole compound solution was taken in a 1 cm path length cuvette and each time 5 μl of DNA was added. Absorption spectra were recorded in the range of 200 nm–400 nm. All the solutions used were freshly prepared before commencing the experiment and titration was carried out until saturation of absorbance occurs.

4.2.7. Fluorescence titration

Fluorescence emission spectra were measured at 25 °C using a Hitachi F7000 spectrofluorimeter (Maryland, USA) using a 1 cm path length quartz cuvette. Quartz cuvettes was thoroughly washed with distilled water and dilute nitric acid (approximately 0.1 N) to minimize non-specific binding of the molecules to the surface of the cuvette. Throughout the fluorescence experiment, concentration of the β-carboline bisindole compounds were kept constant (10 μM) and titrated with increasing concentrations of CT-DNA (multiples of 0.5 μM). Fluorescence spectra were recorded after each addition of CT-DNA to the fluorescent cuvette. The β-carboline bisindole compounds were excited at 305 nm and emission spectra for each titration were recorded from 315 to 600 nm depending upon the molecule. Each spectrum was recorded three times and the average of three scans was taken.

4.2.8. Circular dichroism studies

DNA conformational studies were carried out on a JASCO 815 CD spectropolarimeter (Jasco, Tokyo, Japan). Spectroscopic studies were performed to study the interaction of RT β-carboline bisindole compound with CT-DNA at micro molar concentration range. CT-DNA solution was prepared in 100 mM *Tris*-HCl (pH 7.0). To 10 μM of CT-DNA about 10.0 μM and 20 μM (1:1 and 1:2 ratio of DNA: β-carboline bisindole compound) of each compound solution was added and CD spectra was recorded from 220 nm to 350 nm in a 1 mm path length cuvette. The spectra were averaged over 3 scans.

4.2.9. Viscosity studies

Viscosity experiments were conducted on Ostwald viscometer, immersed in a water bath maintained at 25 °C. Viscosity experiments were performed for each compound (15 μM), after mixing them with CT-DNA solution (150 μM). Before mixing DNA and compounds, viscosity measurements were performed with CT-DNA alone. Et Br-CT-DNA and Hoechst 33342-CT-DNA complexes were considered as control. DNA solution was prepared in 100 mM *Tris*-HCl (pH 7.0). Graph was drawn by plotting $(\eta/\eta_o)^{1/3}$ versus complex/CT-DNA, where η is the viscosity of CT-DNA in the presence of β-carboline bisindole compounds and η_o is the viscosity of CT-DNA alone. Viscosity values were calculated according to the protocol mentioned by Tan et al. [46].

4.3. Molecular docking studies

The molecular docking studies were performed at the M38 binding site of the DNA Topoisomerase I (PDB ID: 1SC7) [47] and 44D binding sites present in 1NAB [48] respectively. The co-ordinates of the crystal structure were obtained from RCSB-Protein Data Bank and suitable corrections to it were made by using Protein Preparation Wizard from Schrödinger package. In regard to the ligands, molecules were constructed using ChemBio3D Ultra 12.0 and their geometries were optimized using molecular mechanics. Finally, docking studies were performed on the most active molecule (**7g** and **7r**) by using AutoDock 4.2 docking software [49] and the results were visualized through PyMOL [50].

Acknowledgements

The authors J.K and B.N are thankful to Department of Science & Technology, New Delhi for providing fellowships under DST-INSPIRE programme.

Appendix A. Supplementary data

Supplementary data related to this article can be found at https://doi.org/10.1016/j.ejmech.2017.10.054.

References

[1] a) L.A. Torre, R.L. Siegel, E.M. Ward, A. Jemal, Global cancer incidence and mortality rates and trends-an update, Cancer Epidemiol. Biomarkers Prev. 25 (2016) 16–27;
b) www.who.int/cancer/media/news/cancer-prevention-resolution/en/.
[2] L.H. Hurley, DNA and its associated processes as targets for cancer therapy, Nat. Rev. Cancer 2 (2002) 188–200.
[3] J. Sheng, J. Gan, Z. Huang, Structure based DNA targeting strategies with small molecule ligands for drug discovery, Med. Res. Rev. 33 (2013) 1119–1173.
[4] K. Dileep, V. Vijeesh, C. Remya, Rational design and interaction studies of combilexins towards duplex DNA, Mol. Biosyst. 12 (2016) 860–867.
[5] H.K. Wang, S.L. Morris-Natschke, K.H. Lee, Recent advances in the discovery and development of topoisomerase inhibitors as antitumor agents, Med. Res. Rev. 17 (1997) 367–425.
[6] A.K. McClendon, N. Osheroff, The geometry of DNA supercoils modulates topoisomerase-mediated DNA cleavage and enzyme response to anticancer drugs, Biochem 45 (2006) 3040–3050.
[7] M. Rueping, C. Vila, Visible light photoredox-catalyzed multicomponent reactions, Org. Lett. 15 (2013) 2092–2095.
[8] D.J. Newman, G.M. Cragg, Natural products as sources of new drugs over the last 25 years, J. Nat. Prod. 70 (2007) 461–477.
[9] J.M. Giulietti, P.M. Tate, A. Cai, B. Cho, S.P. Mulcahy, DNA-binding studies of the natural β-carboline eudistomin U, Bioorg. Med. Chem. Lett. 26 (2016) 4705–4708.
[10] R. Brokamp, B. Bergmann, I.B. Müller, S. Bienz, Stereoselective preparation of pyridoxal 1, 2, 3, 4-tetrahydro-β-carboline derivatives and the influence of their absolute and relative configuration on the proliferation of the malaria parasite Plasmodium falciparum, Bioorg. Med. Chem. 22 (2014) 1832–1837.
[11] K. Patel, M. Gadewar, R. Tripathi, S. Prasad, D.K. Patel, A review on medicinal importance, pharmacological activity and bioanalytical aspects of beta-carboline alkaloid "Harmine", Asian Pac. J. Trop. Biomed. 2 (2012) 660–664.
[12] Y. Wang, J. Shao, S. Yao, S. Zhang, J. Yan, H. Wang, Y. Chen, Study on the antithrombotic activity of Umbilicaria esculenta polysaccharide, Carbohydr. Polym. 105 (2014) 231–236.
[13] K. Yao, M. Zhao, X. Zhang, Y. Wang, L. Li, M. Zheng, S. Peng, A class of oral N-[(1S, 3S)-1-methyl-1, 2, 3, 4-tetrahydro-β-carboline-3-carbonyl]-N′-(amino-acid-acyl) hydrazine: discovery, synthesis, in vitro anti-platelet aggregation/in vivo anti-thrombotic evaluation and 3D QSAR analysis, Eur. J. Med. Chem. 46 (2011) 3237–3249.
[14] F.C. Savariz, M.A. Foglio, A.L.T.G. Ruiz, W.F. da Costa, M. de Magalhães Silva,

J.C.C. Santos, I.M. Figueiredo, E. Meyer, J.E. de Carvalho, M.H. Sarragiotto, Synthesis and antitumor activity of novel 1-substituted phenyl 3-(2-oxo-1, 3, 4-oxadiazol-5-yl) β-carbolines and their Mannich bases, Bioorg. Med. Chem. 22 (2014) 6867–6875.
[15] Y. Song, J. Wang, S.F. Teng, D. Kesuma, Y. Deng, J. Duan, J.H. Wang, R.Z. Qi, M.M. Sim, β-Carbolines as specific inhibitors of cyclin-Dependent kinases, Bioorg. Med. Chem. Lett. 12 (2002) 1129–1132.
[16] A.C. Castro, L.C. Dang, F. Soucy, L. Grenier, H. Mazdiyasni, M. Hottelet, L. Parent, C. Pien, V. Palombella, J. Adams, Novel IKK inhibitors: β-carbolines, Bioorg. Med. Chem. Lett. 13 (2003) 2419–2422.
[17] A. Kamal, M. Sathish, V.L. Nayak, V. Srinivasulu, B. Kavitha, Y. Tangella, D. Thummuri, C. Bagul, N. Shankaraiah, N. Nagesh, Design and synthesis of dithiocarbamate linked β-carboline derivatives: DNA topoisomerase II inhibition with DNA binding and apoptosis inducing ability, Bioorg. Med. Chem. 23 (2015) 5511–5526.
[18] Z. Chen, R. Cao, B. Shi, W. Yi, L. Yu, H. Song, Z. Ren, W. Peng, Synthesis of novel β-carbolines with efficient DNA-binding capacity and potent cytotoxicity, Bioorg. Med. Chem. Lett. 20 (2010) 3876–3879.
[19] S. Li, A. Wang, F. Gu, Z. Wang, C. Tian, Z. Qian, L. Tang, Y. Gu, Novel harmine derivatives for tumor targeted therapy, Oncotarget 6 (2015) 8988–9001.
[20] L.C. Tu, C.-S. Chen, I.-C. Hsiao, J.-W. Chern, C.-H. Lin, Y.-C. Shen, S.F. Yeh, The β-carboline analog Mana-Hox causes mitotic aberration by interacting with DNA, Chem. Biol. 12 (2005) 1317–1324.
[21] A. Kamal, M.N. Rao, P. Swapna, V. Srinivasulu, C. Bagul, A.B. Shaik, K. Mullagiri, J. Kovvuri, V.S. Reddy, K. Vidyasagar, Synthesis of β-carboline–benzimidazole conjugates using lanthanum nitrate as a catalyst and their biological evaluation, Org. Biomol. Chem. 12 (2014) 2370–2387.
[22] A. de Sa, R. Fernando, E.J. Barreiro, M. Fraga, C. Alberto, From nature to drug discovery: the indole scaffold as a 'privileged structure', Mini. Rev. Med. Chem. 9 (2009) 782–793.
[23] C. Bailly, C. Carrasco, F. Hamy, H. Vezin, M. Prudhomme, A. Saleem, E. Rubin, The camptothecin-resistant topoisomerase I mutant F361S is cross-resistant to antitumor rebeccamycin derivatives. A model for topoisomerase I inhibition by indolocarbazoles, Biochem 38 (1999) 8605–8611.
[24] W.-R. Chao, D. Yean, K. Amin, C. Green, L. Jong, Computer-aided rational drug design: a novel agent (SR13668) designed to mimic the unique anticancer mechanisms of dietary indole-3-carbinol to block Akt signaling, J. Med. Chem. 50 (2007) 3412–3415.
[25] J.M. Kelly, A.B. Tossi, D.J. McConnell, C. OhUigin, A study of the interactions of some polypyridylruthenium (II) complexes with DNA using fluorescence spectroscopy, topoisomerisation and thermal denaturation, Nucleic Acids Res. 13 (1985) 6017–6034.
[26] K.T. Chan, F.Y. Meng, Q. Li, C.Y. Ho, T.S. Lam, Y. To, W.H. Lee, M. Li, K.H. Chu, M. Toh, Cucurbitacin B induces apoptosis and S phase cell cycle arrest in BEL-7402 human hepatocellular carcinoma cells and is effective via oral administration, Cancer Lett. 294 (2010) 118–124.
[27] J.-K. Shen, H.-p. Du, M. Yang, Y.-G. Wang, J. Jin, Casticin induces leukemic cell death through apoptosis and mitotic catastrophe, Ann. Hematol. 88 (2009) 743–752.
[28] N. Wu, X.-W. Wu, K. Agama Y, J. Pommier, D. Du, L.-Q. Li, Z.-S. Gu, L.-K. Huang, A novel DNA topoisomerase I inhibitors with different mechanism from camptothecin induces g2/m phase cell cycle arrest to K562 cells, Biochem 49 (2010) 10131–10136.
[29] H. Zhu, J. Zhang, N. Xue, Y. Hu, B. Yang, Q. He, Novel combretastatin A-4 derivative XN0502 induces cell cycle arrest and apoptosis in A549 cells, Investig. New Drugs 28 (2010) 493–501.
[30] E.C. Long, J.K. Barton, On demonstrating DNA intercalation, Acc. Chem. Res. 23 (1990) 271–273.
[31] S. Satyanarayana, J.C. Dabrowiak, J.B. Chaires, Tris (phenanthroline) ruthenium (II) enantiomer interactions with DNA: mode and specificity of binding, Biochemis 32 (1993) 2573–2584.
[32] B.-d. Wang, Z.-Y. Yang, P. Crewdson, D.-q. Wang, Synthesis, crystal structure and DNA-binding studies of the Ln (III) complex with 6-hydroxychromone-3-carbaldehyde benzoyl hydrazone, J. Inorg. Biochem. 101 (2007) 1492–1504.
[33] J. Wu, M. Zhao, K. Qian, K.-H. Lee, S. Morris-Natschke, S. Peng, Novel N-(3-carboxyl-9-benzyl-β-carboline-1-yl) ethylamino acids: synthesis, anti-tumor evaluation, intercalating determination, 3D QSAR analysis and docking investigation, Eur. J. Med. Chem. 44 (2009) 4153–4161.
[34] E. Nyarko, N. Hanada, A. Habib, M. Tabata, Fluorescence and phosphorescence spectra of Au (III), Pt (II) and Pd (II) porphyrins with DNA at room temperature, Inorg. Chim. Acta 357 (2004) 739–745.
[35] N. Shahabadi, S. Kashanian, M. Purfoulad, DNA interaction studies of a platinum (II) complex, PtCl 2 (NN)(NN= 4, 7-dimethyl-1, 10-phenanthroline), using different instrumental methods, Spectrochim. Acta Part A Mol. Biomol. Spectrosc. 72 (2009) 757–761.
[36] H. Fukuda, M. Katahira, N. Tsuchiya, Y. Enokizono, T. Sugimura, M. Nagao, H. Nakagama, Unfolding of quadruplex structure in the G-rich strand of the minisatellite repeat by the binding protein UP1, Proc. Nat. Acad. Sci. 99 (2002) 12685–12690.
[37] V.G. Vaidyanathan, B.U. Nair, Photooxidation of DNA by a cobalt (II) tridentate complex, J. Inorg. Biochem. 94 (2003) 121–126.
[38] C. Metcalfe, C. Rajput, J.A. Thomas, Studies on the interaction of extended terpyridyl and triazine metal complexes with DNA, J. Inorg. Biochem. 100 (2006) 1314–1319.
[39] A. Kamal, V. Srinivasulu, V.L. Nayak, M. Sathish, N. Shankaraiah, C. Bagul, N. Reddy, N. Rangaraj, N. Nagesh, Design and synthesis of C3-Pyrazole/Chalcone-Linked beta-carboline hybrids: antitopoisomerase I, DNA interactive, and apoptosis inducing anticancer agents, Chem. Med. Chem. 9 (2014) 2084–2098.
[40] M. Botta, S. Armaroli, D. Castagnolo, G. Fontana, P. Perad, E. Bombardelli, Synthesis and biological evaluation of new taxoids derived from 2-deacetoxytaxinine, Bioorg. Med. Chem. Lett. 17 (2007) 1579–1583.
[41] T.S. Dexheimer, Y. Pommier, DNA cleavage assay for the identification of topoisomerase I inhibitors, Nat. Protoc. 3 (2008) 1736–1750.
[42] K. Toshima, Y. Okuno, Y. Nakajima, S. Matsumura, β-Carboline–Carbohydrate hybrids: molecular design, chemical synthesis and evaluation of novel DNA photocleavers, Bioorg. Med. Chem. Lett. 12 (2002) 671–673.
[43] M.G. Alvarez, M.S. Arias, M.-J. Fernandez, L. Gude, A. Lorente, G. Alzuet, J. Borras, Pyridine and p-Nitrophenyl oxime esters with possible photochemotherapeutic activity: synthesis, DNA photocleavage and DNA binding studies, Bioorg. Med. Chem. Lett. 18 (2008) 3286–3290.
[44] M. Szumilak, A. Szulawska-Mroczek, K. Koprowska, M. Stasiak, W. Lewgowd, A. Stanczak, M. Czyz, Synthesis and in vitro biological evaluation of new polyamine conjugates as potential anticancer drugs, Eur. J. Med. Chem. 45 (2010) 5744–5751.
[45] L.J. Browne, C. Gude, H. Rodriguez, R.E. Steele, A.J. Bhatnager, Fadrozole hydrochloride: a potent, selective, nonsteroidal inhibitor of aromatase for the treatment of estrogen-dependent disease, J. Med. Chem. 34 (1991) 725–736.
[46] C. Tan, J. Liu, L. Chen, S. Shi, L. Ji, Synthesis, structural characteristics, DNA binding properties and cytotoxicity studies of a series of Ru (III) complexes, J. Inorg. Biochem. 102 (2008) 1644–1653.
[47] B.L. Staker, M.D. Feese, M. Cushman, Y. Pommier, D. Zembower, L. Stewart, A.B. Burgin, Structures of three classes of anticancer agents bound to the human topoisomerase I-DNA covalent complex, J. Med. Chem. 48 (2005) 2336–2345.
[48] C. Temperini, L. Messori, P. Orioli, C.D. Bugno, F. Animati, G. Ughetto, The crystal structure of the complex between a disaccharide anthracycline and the DNA hexamer d (CGATCG) reveals two different binding sites involving two DNA duplexes, Nucleic Acids Res. 31 (2003) 1464–1469.
[49] G.M. Morris, R. Huey, W. Lindstrom, M.F. Sanner, R.K. Belew, D.S. Goodsell, A.J. Olson, AutoDock4 and AutoDockTools4: automated docking with selective receptor flexibility, J. Comput. Chem. 30 (2009) 2785–2791.
[50] W.L. DeLano, The PyMOL Molecular Graphics System, 2002.